

RESEARCH ARTICLE

10.1002/2016JF003859

Key Points:

- Erosion rates from cosmogenic nuclides may be biased when sediment size varies across catchment slopes
- Forward modeling shows that the potential for grain size bias is higher in larger, higher-relief catchments
- Combining cosmogenic nuclides and detrital thermochronometry from multiple sediment sizes helps quantify bias

Correspondence to:

C. E. Lukens,
clukens@uwyo.edu

Citation:

Lukens, C. E., C. S. Riebe, L. S. Sklar, and D. L. Shuster (2016), Grain size bias in cosmogenic nuclide studies of stream sediment in steep terrain, *J. Geophys. Res. Earth Surf.*, 121, 978–999, doi:10.1002/2016JF003859.

Received 12 FEB 2016

Accepted 25 APR 2016

Accepted article online 28 APR 2016

Published online 20 MAY 2016

Grain size bias in cosmogenic nuclide studies of stream sediment in steep terrain

Claire E. Lukens¹, Clifford S. Riebe¹, Leonard S. Sklar², and David L. Shuster^{3,4}

¹Department of Geology and Geophysics, University of Wyoming, Laramie, Wyoming, USA, ²Department of Earth and Climate Sciences, San Francisco State University, San Francisco, California, USA, ³Department of Earth and Planetary Sciences, University of California, Berkeley, California, USA, ⁴Berkeley Geochronology Center, Berkeley, California, USA

Abstract Cosmogenic nuclides in stream sediment are widely used to quantify catchment-average erosion rates. A key assumption is that sampled sediment is representative of erosion from the entire catchment. Here we show that the common practice of collecting a narrow range of sizes—typically sand—may not yield a representative sample when the grain size distribution of sediment produced on slopes is spatially variable. A grain size bias arises when some parts of the catchment produce sand more readily than others. To identify catchments that are prone to this bias, we used a forward model of sediment mixing and erosion to explore the effects of catchment relief and area across a range of altitudinal gradients in sediment size and erosion rate. We found that the bias increases with increasing relief, because higher-relief catchments have a larger fraction of high elevations that are underrepresented in the sampled sand when grain size increases with altitude. The bias also increases with catchment area, because sediment size reduction during transport causes an underrepresentation of more distal, higher elevations within the catchment. Our analysis indicates that grain size bias may be significant at many sites where cosmogenic nuclides have been used to quantify catchment-average erosion rates. We discuss how to quantify and account for the bias using cosmogenic nuclides and detrital thermochronometry in multiple sediment sizes.

1. Introduction

Cosmogenic nuclides have revolutionized research on erosion in mountain landscapes. Until about two decades ago, there were few ways to measure catchment-scale erosion rates over timescales longer than human observation [Kirchner *et al.*, 2001]. Today, cosmogenic nuclides in stream sediment are commonly used to quantify millennial averaged catchment-wide erosion rates [Portenga and Bierman, 2011]. One strength of the approach is that it integrates information about sediment that originates from many points within the catchment [Brown *et al.*, 1995; Bierman and Steig, 1996; Granger *et al.*, 1996]. Thus, it averages over both temporal and spatial variability in erosion rates [e.g., Clapp *et al.*, 2000], which can otherwise obscure the effects of lithology, climate, and tectonics in studies of factors that influence landscape evolution [Riebe *et al.*, 2000, 2001a; Kirchner *et al.*, 2001; Ouimet *et al.*, 2009; Palumbo *et al.*, 2010; Moon *et al.*, 2011; Hahm *et al.*, 2014; Scherler *et al.*, 2014; Fuchs *et al.*, 2015].

Researchers have applied this approach in diverse settings, from slowly eroding Australia and Africa [Bierman and Caffee, 2001; Heimsath *et al.*, 2001, 2010; Chadwick *et al.*, 2013; Bierman *et al.*, 2014] to the rapidly eroding Himalaya [Vance *et al.*, 2003; Wobus *et al.*, 2005; Ouimet *et al.*, 2009; Scherler *et al.*, 2014; Olen *et al.*, 2015], enabling new insights into feedbacks between erosion, climate, and tectonics in long-term landscape evolution [Binnie *et al.*, 2007; Wittmann *et al.*, 2007; Cyr and Granger, 2008; Norton *et al.*, 2008; Abbühl *et al.*, 2010; Moon *et al.*, 2011; DiBiase *et al.*, 2012; Olivetti *et al.*, 2012; Olen *et al.*, 2015; Marshall *et al.*, 2015; Rades *et al.*, 2015; Ferrier *et al.*, 2016]. Erosion rates from cosmogenic nuclides in stream sediment can also shed light on catchment-wide weathering rates [Riebe *et al.*, 2001b, 2003, 2004a; von Blanckenburg *et al.*, 2004; Norton and von Blanckenburg, 2010] and constrain rate constants in geomorphic transport laws, such as nonlinear diffusive transport of sediment across hillslopes [Hurst *et al.*, 2013].

To accurately quantify the average erosion rate of a catchment using cosmogenic nuclides, the sampled stream sediment must be representative of any spatial variations in erosion rates across individual points on catchment slopes. The common practice is to collect sand-sized sediment, even though the eroded material ranges in size from clay to boulders in many of the streams and rivers where the approach has been applied. Although it has not been widely recognized in the literature, sampling a narrow range of sediment sizes implicitly assumes that

it represents the same fraction of the sediment size distribution across all sediment sources in the catchment. This condition is satisfied when the sediment size distribution is spatially uniform. However, there are many reasons why grain size distributions might vary across slopes. Differences in hillslope angle, climate, vegetation, and bioturbation can all drive variations in weathering and erosion [White and Blum, 1995; Gabet, 2000; Roering *et al.*, 2010; Hahm *et al.*, 2014] that may cause variations in sediment size across catchments [Attal *et al.*, 2015; Marshall and Sklar, 2012; Riebe *et al.*, 2015]. For instance, steeper slopes may be more vulnerable to landsliding [e.g., Dietrich *et al.*, 1995] and thus could produce coarser grain sizes [Casagli *et al.*, 2003; Attal *et al.*, 2015]. Lower elevations may experience warmer average temperatures and be more susceptible to chemical weathering [Drever and Zobrist, 1992; Riebe *et al.*, 2004b], thus producing finer sediment [Riebe *et al.*, 2015].

Although few studies have quantified how sediment size varies across slopes within an individual catchment, mounting evidence suggests that it may introduce biases in cosmogenic nuclide studies of mountain catchments: Different grain sizes in mountain streams often harbor different cosmogenic nuclide concentrations. These differences have been interpreted to reflect preferential sourcing of coarse sediment from subsurface depths that are more deeply shielded from cosmic rays [Brown *et al.*, 1995; Belmont *et al.*, 2007]; preferential breakdown of coarse material from higher-elevation slopes where cosmogenic nuclide production rates are higher [Matmon *et al.*, 2003; Belmont *et al.*, 2007; Puchol *et al.*, 2014] and differences in the timescales of sediment transport and nuclide accumulation across slopes [Carretier *et al.*, 2009; Codilean *et al.*, 2010, 2014; Vassallo *et al.*, 2011; Aguilar *et al.*, 2014]. However, such differences can also arise when the sizes of sediment produced by weathering and erosion vary across slopes in a catchment. For instance, if areas that erode relatively slowly also produce relatively more sand and less gravel, samples of sand would have higher nuclide concentrations than samples of gravel, solely due to the slower erosion rates in the areas that produce most of the sand. Moreover, both the sand and the gravel would preferentially represent erosion from different parts of the catchment, and neither size would likely have a nuclide concentration that reflects the catchment-average erosion rate. In general, the average cosmogenic nuclide concentration in any narrow range of sediment sizes might be lower or higher than the true catchment average, leading to estimates of catchment-average erosion rates that are either too high or too low. Thus, spatial variations in the sizes of sediment produced on slopes can lead to bias in estimates of erosion rates derived from a narrow range of sediment sizes.

Observations of cosmogenic nuclides in sediment from Inyo Creek, California, suggest that the bias can be significant: Using only sand in a ^{10}Be estimate of catchment-average erosion rate leads to a factor of ~ 3 bias due to spatial variations in the size distribution of sediment produced on slopes [Riebe *et al.*, 2015]. In comparison, propagated uncertainties in erosion rates inferred from ^{10}Be are typically less than 9% and replicate analyses from the same grain sizes typically agree to within 30% [e.g., Bierman *et al.*, 1999; Matmon *et al.*, 2003; Clapp *et al.*, 2002; Binnie *et al.*, 2006; Ouimet *et al.*, 2009; DiBiase *et al.*, 2010]. The potential for grain size bias in cosmogenic nuclide studies raises a series of questions about measurements that have been based on a narrow range of sediment sizes: Under what circumstances (i.e., in which landscapes) will erosion rates be overestimated or underestimated? How big might the bias be? What can be done to minimize or account for the bias?

Here we address these questions using a forward model that tracks the evolution of cosmogenic nuclide concentrations in each grain size from sediment sources on catchment slopes to the sampling point in the stream. In the model, each elevation in the landscape has an adjustable erosion rate and grain size distribution of sediment produced by weathering and erosion. Sediment from each point is mixed with sediment from other sources into an aggregate that can be sampled at the catchment mouth. We can query this aggregate for the average nuclide concentrations of the different grain sizes and thus evaluate the potential for bias due to spatial variations in both the erosion rate and grain size distribution of sediment produced on slopes.

To explore the sensitivity of the bias to differences in weathering and erosion, we simulated different changes in grain size distribution and erosion rate across the Inyo Creek catchment, where altitudinal gradients in slope, climate, and vegetation contribute to altitudinal differences in sediment size [Riebe *et al.*, 2015]. We found that steeper altitudinal increases in both erosion rate and average grain size produce larger biases in cosmogenic-based estimates of catchment-average erosion rates. We also explored the potential for grain size bias in other landscapes using self-similar synthetic catchments that allow us to vary catchment relief and area across a range of conditions in which cosmogenic nuclides have been measured. We found that the bias increases with total catchment relief when grain size increases with elevation. The bias also increases with catchment area due to the modeled effects of sediment size reduction during downstream transport. The

largest biases arise in large, high-relief catchments in which mean grain size and erosion rate both increase quickly with elevation. Conversely, relatively little bias occurs in small, low-relief catchments with low altitudinal gradients in grain size.

2. Modeling Spatial Variations in Grain Size and Erosion Rates

Our goal was to explore how cosmogenic nuclides in stream sediment are influenced by variations in the sizes of sediment produced on hillslopes. To accomplish this, we built on the conventional model of sediment and nuclide mixing that has been used to evaluate catchment-average erosion rates for over 20 years [Brown *et al.*, 1995; Granger *et al.*, 1996; Bierman and Steig, 1996]. Before discussing the modifications employed in our analysis, we outline the conventional framework below.

Beginning at any point (i) on a catchment slope, the cosmogenic nuclide concentration (N_i) of a host mineral in sediment produced by hillslope erosion should be inversely proportional to the local erosion rate (E_i) as shown in equation (1).

$$N_i = \frac{P_i \Lambda}{E_i}. \quad (1)$$

Here P_i is the local production rate of the cosmogenic nuclide in the host mineral, and Λ is a scaling factor for the decrease in production rates with depth below the surface. Equation (1) assumes that radioactive decay of the cosmogenic nuclide is negligible [e.g., Lal, 1991]. This assumption introduces errors that are significantly smaller than the grain size bias because the averaging timescale of erosion (i.e., Λ/E) is small compared to the radioactive mean lives of ^{10}Be and ^{26}Al for the range of erosion rates considered here.

If each point contributes cosmogenic nuclides to stream sediment in direct proportion to the local erosion rate and the local area of the point (A_i), then the average nuclide concentration in a host mineral in the stream sediment ($\langle N \rangle$) should be an area-weighted and erosion-rate-weighted average of the nuclide concentrations from each point:

$$\langle N \rangle = \frac{\sum N_i E_i A_i}{\sum E_i A_i}. \quad (2)$$

In our analyses, A_i is a constant equal to the area of each pixel in a digital elevation model (DEM), E_i is assigned to each pixel using an imposed relationship between erosion rate and altitude, and N_i is calculated from E_i using equation (1).

Combining equations (1) and (2) and rearranging the terms yield equation (3):

$$\langle E \rangle = \frac{\langle P \rangle \Lambda}{\langle N \rangle}. \quad (3)$$

The catchment-average erosion rate $\langle E \rangle$ is proportional to the catchment-average nuclide production rate ($\langle P \rangle$) and inversely proportional to the average nuclide concentration in the stream sediment [Brown *et al.*, 1995; Granger *et al.*, 1996; Bierman and Steig, 1996].

Equations (2) and (3) implicitly assume that the sampled sediment is representative of the mixture of sediment in the stream. However, this assumption requires that either the size distribution of eroded sediment does not vary from point to point across catchment slopes, or that the sampled stream sediment is representative of erosion despite any spatial variability in sediment size. Quantifying variability in eroded sediment size across slopes remains a fundamental challenge [Attal and Lavé, 2006; Marshall and Sklar, 2012; Attal *et al.*, 2015; Riebe *et al.*, 2015]. Thus, it is difficult to know a priori whether the cosmogenic nuclide concentration in any one sampled size (or combination of sizes) accurately records the catchment-average erosion rate. In the next section, we introduce a series of scenarios in which sediment size and erosion rates vary across plausible ranges, and explain in conceptual terms how these variations lead to bias in measurements of catchment-average erosion rates.

2.1. Conceptual Model for Grain Size Bias

In the simple case where neither the erosion rate nor the grain size distribution varies across sediment sources on slopes, each source should contribute equally to a sample of any given sediment size collected

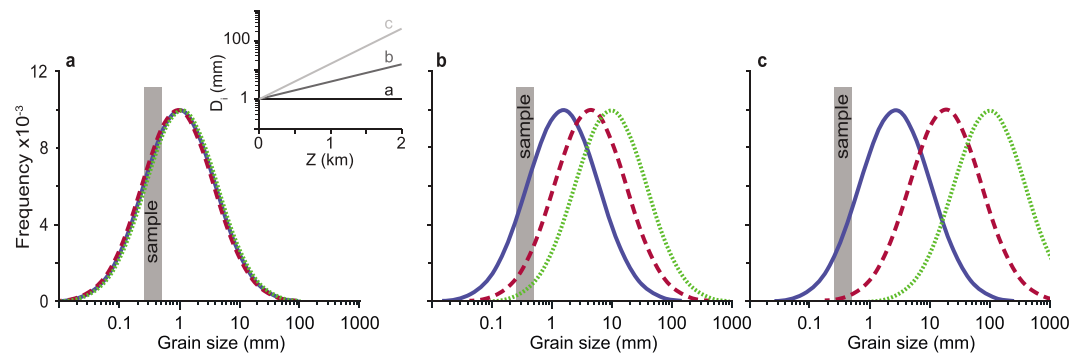


Figure 1. Conceptual model illustrating how grain size bias arises when higher elevations are underrepresented in sampled sediment. Inset shows altitudinal increase in median sediment size (D_i) for scenarios in main panels. (a) The size distribution of sediment on hillslopes at low elevations (blue solid line), midelevations (red dashed line), and high elevations (green dotted line) is the same. Any sampled sediment size (e.g., vertical gray bar) will contain the same fraction of the overall size distribution from each elevation. (b) Sediment size increases with altitude such that the fractional contribution of sand from higher elevations will be smaller in a sample collected at the catchment outlet. Thus, the contribution from erosion at higher elevations will be underrepresented in the sample, leading to a bias toward erosion rates at lower elevations. (c) Sediment size increases more quickly with altitude, such that the middle and high elevations are more underrepresented in the sample, resulting in a larger bias.

from the stream (Figure 1a). Any sample of well-mixed stream sediment could therefore be used to infer the catchment-average erosion rate using equation (3). Complications arise when sediment size changes across the catchment, because each sediment size can reflect a different fraction of the erosion occurring at each point on the landscape. For example, if grain size increases with elevation, lower elevations will tend to contribute a higher fraction of the sand-sized sediment typically sampled from streams in cosmogenic nuclide studies of erosion rates (Figure 1b). Higher elevations would be underrepresented in the sample, and thus, nuclide concentrations in the host mineral would be biased toward lower elevations. This effect would be amplified by steeper altitudinal increases in sediment size (Figure 1c).

Figure 1 illustrates the challenge of collecting sediment that is representative of erosion in catchments where sediment size varies across slopes. The implications of misrepresenting some parts of the catchment in a sample can be profound, introducing significant bias in some cosmogenic nuclide studies of erosion. The sense of bias—i.e., whether the estimated erosion rate is too high or too low—depends on the spatial distribution of erosion rates across the catchment. For example, in the simple case where erosion rates are spatially uniform and sediment size increases with elevation as shown in Figure 2a, the average nuclide concentration in a sample of sand will be lower than the true spatially averaged nuclide concentration (Figure 2b), and equation (3) will overestimate the catchment-average erosion rate. Here a bias arises because nuclide production rates, and thus nuclide concentrations, increase with sediment source elevation (Figures 2a and 2b). Because nuclide production rates are affected by the attenuation of secondary cosmic rays in Earth's atmosphere, higher elevations have higher production rates and thus higher nuclide concentrations for a given erosion rate (see equation (1)). If high elevations are underrepresented in the sampled sediment, catchment-average erosion rates inferred from equation (3) will be too high, even when erosion rates are spatially uniform.

If erosion rates increase with elevation, the altitudinal increase in nuclide concentrations would be less steep (Figure 2c) because of the trade-off between rates of erosion and nuclide production in equation (1). Thus, the average nuclide concentration in a sand-sized sample would be closer to the true average, and the bias in the estimated average erosion rate would be smaller. However, the altitudinal increase in erosion rate could be sufficiently steep that its effects on the cosmogenic nuclide concentration at any point on the landscape would overwhelm the effects of increasing production rate with increasing elevation. Because the cosmogenic nuclide concentration is inversely proportional to the local erosion rate (equation (1)), the local nuclide concentration would decrease with elevation, and the average nuclide concentration in a sample of sand would be higher than the true spatially averaged nuclide concentration (Figure 2d). In that case, equation (3) would underestimate the catchment-average erosion rate. Conversely, if erosion rates decreased with elevation, estimated erosion rates from equation (3) would be too high because the sediment with high nuclide concentrations would be underrepresented in the sampled sand.

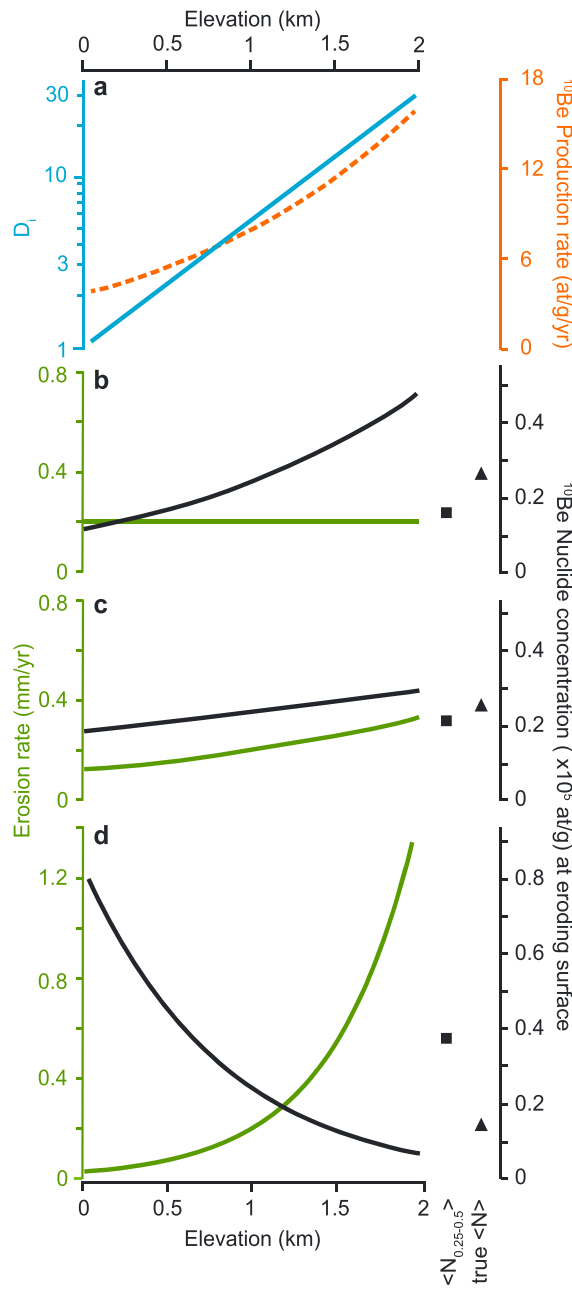


Figure 2. Results from a simple numerical model illustrating grain size bias in cosmogenic nuclide concentrations. (a) The cosmogenic nuclide production rate (orange line) and the median size of eroded sediment (blue line) both increase exponentially with altitude. These relationships are model inputs for the scenarios shown in panels (b and d). (b) When erosion rates are spatially uniform (green line), cosmogenic nuclide concentrations increase with altitude (black line) due solely to increasing nuclide production rates. The average nuclide concentration in sand (square) will be lower than the true average concentration (triangle), and erosion rates estimated from equation (3) will be too high. (c) If erosion rates increase gently with altitude (green line), nuclide concentrations will be relatively uniform across the catchment (black line) and the average concentration in sand will be closer to the true average than in Figure 2b. (d) If erosion rates increase quickly enough with altitude (green line), cosmogenic nuclides will decrease with elevation (black line), such that the average nuclide concentration in sand will be higher than the true average, and the inferred catchment-average erosion rate will be too low.

2.2. Modified Model of Sediment Mixing

To quantify biases that may arise in using a single grain size and equation (3) (Figures 1 and 2), we calculated average nuclide concentrations in each sediment size ($\langle N_\varphi \rangle$) using equation (4).

$$\langle N_\varphi \rangle = \frac{\sum_i N_i E_i A_i f_{\varphi,i}}{\sum_i E_i A_i f_{\varphi,i}} \quad (4)$$

Here $f_{\varphi,i}$ represents the fraction of the sediment eroded from each point (i) on the landscape in a grain size of interest (φ) relative to the total mass of sediment produced at that point. According to equation (4), the average nuclide concentration in each grain size is weighted not only by the erosion rate and local area of the point (as in equation (2)) but also by the fraction of eroded sediment in the sampled size at each point on the landscape. Points that do not produce any sediment in the sampled grain size have $f_{\varphi,i}$ equal to zero and thus will contribute no cosmogenic nuclides to the sample. Conversely, points that produce only the sampled grain size will have $f_{\varphi,i}$ equal to one and thus will contribute all of their nuclides to the mixed sediment from which the sample is taken. By summing over all points, equation (4) mixes sediment from across the entire catchment and yields an estimate of the average nuclide concentration in each grain size ($\langle N_\varphi \rangle$). In our simulations, we used the size-specific average for 0.25–0.5 mm ($\langle N_{0.25-0.5 \text{ mm}} \rangle$) instead of $\langle N \rangle$ in equation (3) to calculate an apparent erosion rate and thus evaluate the magnitude of bias that arises when fine sand is used in equation (3) to estimate catchment-average erosion rates.

Figures 1 and 2 illustrate how bias arises for a simple catchment in which area is distributed evenly across all elevations. Equation (4) can also be applied to elevation distributions from actual DEMs, to explore the implications of grain size

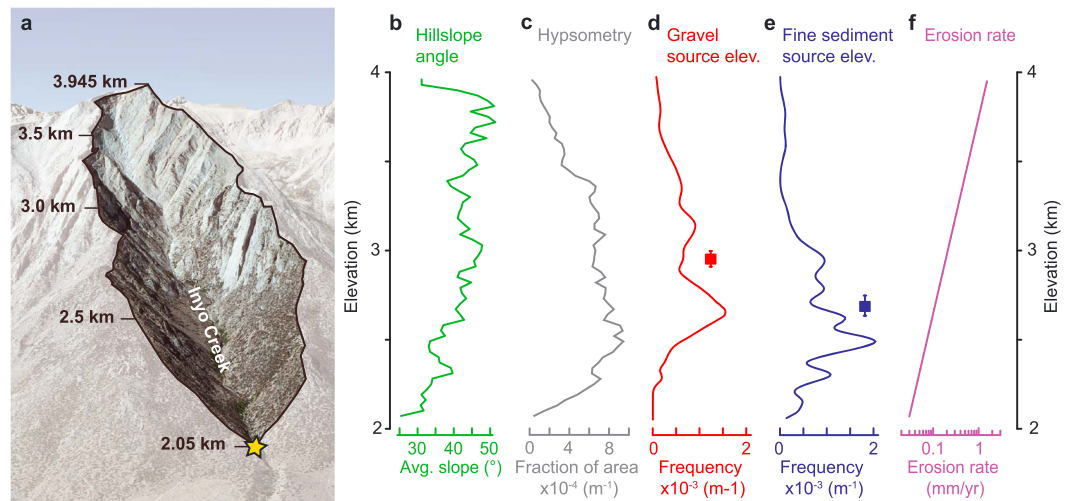


Figure 3. (a) In the steep, 2 km relief catchment drained by Inyo Creek, California, vegetation cover decreases and (b) hillslope angle increases markedly with elevation. (c) The distribution of elevations across the catchment does not closely match the distribution of source elevations for either (d) gravel or (e) finer sediment, suggesting spatial variability in sediment size across the catchment [Riebe *et al.*, 2015]. Source elevations in Figures 3d and 3e are inferred from thermochronometry in stream sediment collected from the sample location (star in a) (fine sediment: Stock *et al.* [2006] and gravel: Riebe *et al.* [2015]). On average, gravel originates from higher elevations than the finer sediment (symbols in Figures 3d and 3e show mean \pm s.e.m (standard error of mean)), indicating that sediment size increases with elevation. Together, source elevations and cosmogenic nuclide measurements from previous work [Stock *et al.*, 2006; Riebe *et al.*, 2015] imply that erosion rates increase quickly with elevation across the catchment. (f) An optimization analysis yielded the best fit exponential increase in erosion rates after Riebe *et al.* [2015], which is used in our forward model.

variations across landscapes where cosmogenic nuclides have been measured in stream sediment. By specifying how erosion rates, sediment sizes, and nuclide production rates vary across slopes, we assigned E_i , P_i , and $f_{\phi,i}$ to each point in the DEM. This allowed us to calculate the distribution of N_i across slopes, which we combined into a catchment-average nuclide concentration for each size class ($\langle N_{\phi} \rangle$) using equation (4). We then calculated the erosion rate we would infer from the 0.25–0.5 mm size class and compared it to the average erosion rate imposed in our model. Thus, we quantified the bias introduced by the conventional practice of sampling a narrow range of sizes. By imposing plausible variations in sediment size and erosion rates across the DEM, we were able to address the question: Under what circumstances is grain size bias likely to arise?

3. Grain Size Bias at Inyo Creek

To illustrate our approach, we applied it to Inyo Creek, California (Figure 3a), where both sediment size and erosion rate vary across catchment slopes [Riebe *et al.*, 2015]. Inyo Creek drains a steep catchment of the eastern Sierra Nevada, where hillslope angle, climate, and vegetation all change substantially over the 2 km of relief from the catchment outlet to the top of Lone Pine Peak (Figures 3a–3c). Apatite (U-Th)/He ages in bedrock increase with elevation at this location [House *et al.*, 1997; Stock *et al.*, 2006].

Ages measured in sediment grains correspond to the bedrock ages at their source elevations on catchment slopes [Stock *et al.*, 2006; Vermeesch, 2007; Riebe *et al.*, 2015]. Age distributions from two different size classes collected from the creek demonstrate that the coarser sediment originates from higher elevations than finer sediment on average (Figures 3d and 3e). Meanwhile, cosmogenic nuclide concentrations are lower in the coarser sediment [Stock *et al.*, 2006; Riebe *et al.*, 2015]. Together these data indicate that erosion rates increase quickly with elevation [Riebe *et al.*, 2015] (Figure 3f).

Because cosmogenic nuclide concentrations differ between sediment sizes, sampling any one sediment size from Inyo Creek will likely result in a biased estimate of the catchment-average erosion rate. How big could the bias be? Spatial variations in erosion rate and sediment size should both influence the bias (Figures 1 and 2) and it is instructive to consider their effects in isolation. To illustrate the effects of variable

sediment size, we needed to first specify a functional relationship between grain size and elevation. In this case we used the following expression:

$$D_i = D_{\min} e^{d(Z_i - Z_0)}. \quad (5)$$

Here D_i is the median grain size, Z_i is the elevation at each point, and D_{\min} is the median grain size at the lowest elevation (Z_0) in the catchment. In our simulations, we held the median grain size at the lowest elevation constant at 1 mm and explored the effects of increasing d , the exponential slope in equation (5), from 0 to 0.0035 m^{-1} . This produced a realistic range of median grain sizes from the bottom of the catchment to the top (largest range = 1–760 mm; Figure 4a). We expected the steeper altitudinal gradients in sediment size to produce larger biases.

We calculated the magnitude of the bias as the ratio between the modeled average erosion rate (E_{avg}) and $E_{0.25-0.5}$, which is the erosion rate inferred from equation (3) using the cosmogenic nuclide concentration in 0.25–0.5 mm stream sediment. Erosion rate can be overestimated or underestimated, reflecting the sense of the bias. To quantify the magnitude of bias, we define the “error factor,” which is always expressed as a value greater than 1 (equation (6)).

$$\begin{aligned} \text{error factor} &= E_{\text{avg}}/E_{0.25-0.5} & \text{if } E_{\text{avg}} > E_{0.25-0.5} \\ \text{error factor} &= E_{0.25-0.5}/E_{\text{avg}} & \text{if } E_{\text{avg}} < E_{0.25-0.5} \end{aligned} \quad (6)$$

Because the error factor is always a positive number greater than 1, it expresses the magnitude of bias independently of the sense of bias—i.e., whether the erosion rate is overestimated or underestimated. For example, if E_{avg} is 0.2 mm/yr and $E_{0.25-0.5}$ is 0.1 mm/yr, the catchment-average erosion rate is underestimated by a factor of 2 (and the error factor is equal to 2). Conversely, if E_{avg} is 0.05 mm/yr and $E_{0.25-0.5}$ is 0.1 mm/yr, the catchment-average erosion rate is overestimated by a factor of 2; the error factor is still 2, but the sense of bias has changed. If E_{avg} equals $E_{0.25-0.5}$, there is no bias, and the error factor equals 1.

Our decision to use a variable definition of error factor (equation (6)) has the potential to introduce confusion. To justify it, we stress that if error factor were instead always calculated in the same way, regardless of the sense of bias, then it would introduce potential for misinterpretation of the relative magnitude of the bias for different scenarios. For example, if error factor were always calculated as $E_{0.25-0.5}/E_{\text{avg}}$, then a bias that caused us to underestimate erosion rates by a factor of 5 would be associated with an error factor of 0.2. Meanwhile, a bias that caused us to overestimate erosion rates by a factor of 5 would be associated with an error factor of 5. According to our preferred variable definition in equation (6), the error factor would be 5 in both cases. Thus, equation (6) avoids inconsistencies in the reported magnitude of bias when the sense of the bias changes. It is therefore also agnostic about whether an underestimate or an overestimate in erosion rate is bigger and thus more of a cause for concern in analyses of catchment-average erosion rates.

3.1. Accounting for Variations in Erosion Rates and Sediment Size

Figure 4 shows how the calculated error factor changed when we varied sediment size and erosion rate at Inyo Creek. For simplicity, we considered just two erosion rate scenarios, one in which they are spatially uniform, and one in which they increase exponentially with elevation. In both scenarios, we explored different spatial variations in median sediment size by changing the coefficient d in equation (5). We found that there is no bias (error factor = 1) if sediment size does not change across the catchment, because $f_{0.25-0.5 \text{ mm}, j}$ is uniform across the landscape and thus has equal weight in each term of the sum in equation (4) (as illustrated in Figure 1a). However, when erosion rates are uniform and sediment size increases with elevation, the error factor increases from 1 to 1.3 with increasing altitudinal gradients in sediment size (Figure 4b). Erosion rates are overestimated because the fine sediment in the sample underrepresents the upper parts of the catchment, where nuclide production rates are faster. Thus, the nuclide concentration in the sampled fine sediment is lower than the average concentration in all sediment sizes leaving the catchment, violating the assumptions of equations (2) and (3). Under this condition, steeper altitudinal increases in grain size result in greater overestimation of erosion rates (Figure 4b), because the sampled sediment has an increasingly smaller fraction of the sediment eroded from high elevations.

The bias has the opposite sense when erosion rates are not spatially uniform but instead increase with elevation: Catchment-average erosion rates are underestimated—not overestimated—from cosmogenic nuclides in the sampled 0.25–0.5 mm sand (Figure 4b). The bias increases for steeper altitudinal increases in grain size, from an error factor of 1 to 3.2 across the range of conditions considered here (Figure 4b). The sense of the bias differs because the altitudinal increase in erosion rates—which makes cosmogenic nuclide concentrations lower at higher elevations—outpaces the altitudinal increase in production rate, which makes

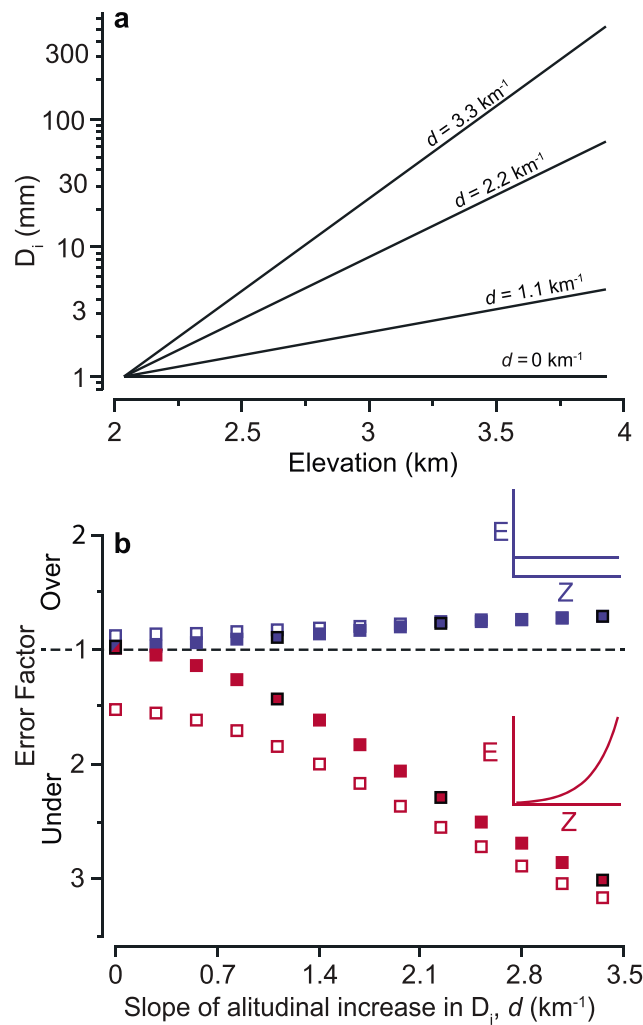


Figure 4. Forward modeling of erosion and sediment mixing showing potential for bias at Inyo Creek. (a) A subset of the altitudinal increases in sediment size used as inputs in the model. (b) Degree to which erosion rates are overestimated or underestimated for different altitudinal increases in sediment size. Points that plot above an error factor of 1 (i.e., “over”) show scenarios in which erosion rates would be overestimated using cosmogenic nuclides measured in sand alone; points that plot below an error factor of 1 (i.e., “under”) show scenarios in which erosion rates would be underestimated. The slopes of lines in Figure 4a correspond to the horizontal axis in Figure 4b, and symbols outlined in black in Figure 4b correspond to the lines plotted in Figure 4a. Blue symbols correspond to bias introduced when erosion rates are spatially uniform. Red symbols correspond to bias introduced when erosion rates increase exponentially with altitude according to relationship shown in Figure 3f. Filled symbols show outcomes for erosion with $\alpha = 0 \text{ m}^{-1}$ (i.e., negligible sediment breakdown during transport downstream—see text). Open symbols show outcomes when $\alpha = 0.0002 \text{ m}^{-1}$.

$$D = D_0 e^{-\alpha L} \tag{7}$$

Here D_0 is the initial particle diameter, and α is the exponential breakdown coefficient with dimensions of one over length [Krumbein, 1941; Kodama, 1994]. In our forward model, the final grain size distribution in the stream is set by the areally and erosionally weighted mixture of input sizes (equation (4)) as modified only by sediment breakdown (equation (7)); it does not reflect any preferential transport or fluvial sorting processes [e.g., Gasparini et al., 1999, and references therein].

cosmogenic nuclide concentrations higher at higher elevations. Higher elevations thus produce sediment with lower nuclide concentrations, which are underrepresented in finer sediment sizes in the stream due to the altitudinal increase in grain size. The sampled stream sediment will thus have a higher cosmogenic nuclide concentration than the true catchment average, and erosion rates calculated in the conventional way (using equation (3)) will be too low. Because the altitudinal change in erosion rates at Inyo Creek is fast relative to the altitudinal change in production rates, the bias is much larger when sediment size and erosion rate both increase with altitude (red symbols in Figure 4b) than when sediment size changes alone (blue symbols in Figure 4b). This leads to errors that can be greater than a factor of three for steep altitudinal increases in D_i and erosion rates at Inyo Creek.

3.2. Adding the Effects of Breakdown

We expanded our analysis to include the effects of sediment breakdown during transport, which we have excluded from the discussion thus far. Previous workers have hypothesized that size reduction of sediment during transport to the outlet may introduce variations in cosmogenic nuclide concentrations across sediment sizes [Matmon et al., 2003; Belmont et al., 2007]. Breakdown may play an especially important role in larger catchments with longer travel distances. Breakdown can be described as a reduction in particle diameter (D) in proportion to the distance traveled (L).

The reduction in particle diameter captured in equation (7) results in a loss of mass and thus also cosmogenic nuclides, such that the number of cosmogenic nuclides in a sediment particle after breakdown (n) is given by equation (8).

$$n = n_0 e^{-3\alpha L}. \quad (8)$$

Here the constant 3 in the exponential term scales the decrease in diameter to a decrease in volume and thus mass. The variable n_0 is the number of cosmogenic nuclides that were present in the particle before breakdown, which can be calculated using equation (9).

$$n_0 = \frac{N_i \rho \pi}{6} D_0^3. \quad (9)$$

Equation (9) assumes that the particle is spherical and has a density of ρ . To incorporate equations (7) and (8) into our analysis, we assumed that particles lose mass by abrasion [e.g., Sklar and Dietrich, 2001], which creates silt-sized or smaller byproducts. Because silt is smaller than sizes typically sampled for cosmogenic nuclide measurements, the byproducts of abrasion were not considered in our analysis.

Our results show that breakdown increases the magnitude of bias, regardless of the sense of bias, when sediment size increases with altitude (Figure 4b). However, the bias due to breakdown is smaller when erosion rates are spatially uniform than when erosion rates increase with altitude. In both scenarios, the bias due to breakdown becomes an increasingly smaller fraction of the total bias as the altitudinal gradient in sediment size increases. Breakdown increases bias because it has a greater effect on sediment particles that travel longer distances. In general, higher headwater elevations in a catchment produce sediment that has to travel farther, making them more underrepresented in sediment sampled from the catchment mouth. For a moderate breakdown coefficient ($\alpha = 0.0002 \text{ m}^{-1}$), we calculate that almost all the material in the 0.25–0.5 mm range would be broken down to less than 0.25 mm during transport over the longest travel distances at Inyo Creek.

The loss of nuclides due to the breakdown of 0.25–0.5 mm particles is partly offset by additions from coarser sediment sizes that break down into the sampled 0.25–0.5 mm range. The offset is only partial because all sizes of sediment from high elevations (which travel long distances) are substantially reduced in mass and thus in nuclides (equation (8)). Thus, the contribution from the next larger size class is smaller than the loss of nuclides due to abrasion of particles that started out in the 0.25–0.5 mm size class. The net effect of breakdown is that higher elevations are underrepresented in the analyzed sample.

The decrease in the relative importance of breakdown from left to right in Figure 4b reflects the increasing importance of the altitudinal gradient in sediment size across slopes. As this gradient increases, the 0.25–0.5 mm sand constitutes an increasingly small fraction of the initial size distribution at high elevations. When there is very little fine sand to begin with at high elevations, those elevations will be underrepresented in the sample even when the breakdown coefficient is negligible. Thus, breakdown accounts for an increasingly small fraction of the bias as the gradient in sediment size increases. For example, when sediment size does not increase with elevation (i.e., the altitudinal gradient is zero), the error factor is 1.1 and breakdown accounts for 100% of the bias. In contrast, for the steepest gradient shown in Figure 4b, we estimate an error factor of 3.15, with breakdown contributing only 4.4% of the total bias.

The calculated magnitude of the breakdown effect is controlled by the choice of the breakdown coefficient (α) in equations (7) and (8). We chose an α value of 0.0002 m^{-1} because it falls roughly in the middle of published estimates for breakdown coefficients in field settings [e.g., Sklar *et al.*, 2006; Sklar and Dietrich, 2008]. This value is higher than most estimates of α in experimental studies, which are expected to be at least an order of magnitude lower than field settings [Kodama, 1994; Lewin and Brewer, 2002; Attal and Lavé, 2009]. Although the true breakdown coefficient (α) of sediment in Inyo Creek is unknown, our choice is, if anything, a bit high. Thus, the actual effect of breakdown at Inyo Creek may be smaller than reported here. The overall magnitude of the bias due to breakdown will differ according to both the choice of α and the choice of catchment, due to differences in the distributions of elevation and travel distance. Thus, our analysis from Inyo Creek is somewhat limited in that it only illustrates the direction and possible magnitude of bias imposed by the breakdown effect in a few plausible circumstances.

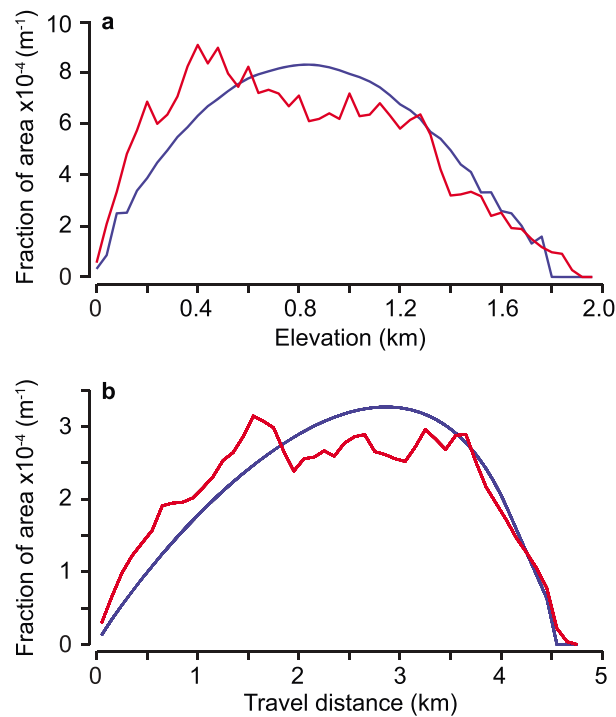


Figure 5. Synthetic (blue) distributions of (a) elevation and (b) travel distance based on parameters listed in Table A1 are broadly similar to the actual distributions (red) generated from a 10 m DEM of Inyo Creek.

given altitudinal gradient in sediment size, because the range in sediment sizes from headwaters to outlet is larger. Likewise, we expect a bigger bias in catchments with larger area, because larger area corresponds to longer travel distances over which sediment can break down to smaller sizes. Catchment shape may also be a factor; the potential for bias should be bigger when more area is at higher elevations, because a larger fraction of the catchment area would be underrepresented in the sample. Thus, relief, area, and shape could all play roles in the potential for bias in catchment-average erosion rates due to spatial variations in sediment size and breakdown during transport.

To quantify the relative importance of relief, area, and shape in the bias, we explored the effects of each factor in isolation, recognizing that they can influence the bias in different ways. For consistency, it might make sense to use DEMs of different-sized catchments from the region around Inyo Creek in our forward model of sediment mixing and breakdown. In practice, however, it is difficult to choose catchments from any location (including the east side of the Sierra Nevada) that span a range in one factor (e.g., relief) without variations in the others (i.e., area and shape). To overcome this limitation, we derived realistic distributions of elevation and travel distance—the two factors that drive the bias in equations (4) and (8)—from a synthetic catchment that can be manipulated to isolate relief, area, and shape as factors of interest.

4.1. Generating Synthetic Distributions of Elevation and Travel Distance

To generate realistic distributions of elevation and travel distance for different-sized catchments, we used well-known scaling relationships from the literature. Beginning with the relationship between area and travel distance (Hack's Law) [Hack, 1957; Rigon *et al.*, 1996] and the relationship between slope and area (Flint's Law) [Flint, 1974], we calculated a channel long profile (Appendix A) [Whipple and Tucker, 1999; Sklar *et al.*, 2016]. This defines the lowest elevation at each travel distance in the catchment. Although there is no similar approach for defining the highest elevation at each travel distance (i.e., the ridge profile), we approximated it in our analysis with a power-law scaling relationship between travel distance and elevation (Appendix A) [Sklar *et al.*, 2016]. Thus, we defined both the upper and lower boundaries of the distribution of elevations at each travel distance. We then used a best fit beta distribution to spread the area at each travel distance across the range of elevations between the channel and the ridge [Sklar *et al.*, 2016]. When applied across

4. Bias in Other Landscapes

Our forward model of sediment mixing at Inyo Creek demonstrates that cosmogenic nuclide concentrations in stream sediment are sensitive to spatial variations in the sizes of sediment produced on hillslopes. Meanwhile, our predictions of the effects of breakdown are consistent with previous work showing that size reduction of sediment during transport to the outlet can influence cosmogenic nuclide concentrations [Matmon *et al.*, 2003; Belmont *et al.*, 2007]. Thus, we have demonstrated that both sediment breakdown and variations in initial sediment size can lead to substantial grain size bias in estimated catchment-average erosion rates.

The observed bias at Inyo Creek, which has high relief but relatively small catchment area, raises the question: how might the bias vary with topography across other landscapes? We expect a bigger bias in catchments with higher relief for a

the entire catchment, our approach yields a modeled distribution of elevations at each travel distance. These distributions can be integrated across all travel distances to yield the distribution of elevation of the catchment (Figure 5a), also known as catchment hypsometry [e.g., Strahler, 1952]. Likewise, the distribution of travel distances can be integrated across all elevations to yield the catchment's travel distance distribution (Figure 5b), also known as the width function [e.g., Shreve, 1969; Troutman and Karlinger, 1984]. The synthetic distributions of elevation and travel distances correspond closely to observed hypsometry and width functions from a DEM of Inyo Creek (Figure 5), demonstrating that our approach yields realistic results. Because our synthetic catchments are based on scaling relationships that have parameters corresponding to catchment relief, area, and shape, we were able to vary the parameters and thus realistically simulate the range of conditions in which cosmogenic nuclides have been used to estimate catchment-average erosion rates. Thus, we were able to explore how the potential for bias varies across natural landscapes.

4.2. Effects of Difference in Relief

To illustrate how relief can influence the potential for bias that arises from spatial variations in sediment size, we compared two synthetic catchments. The first had 1850 m of total catchment relief, similar to Inyo Creek. The second had a much lower relief of 834 m (Figure 6a). For simplicity, we started by ignoring the effects of breakdown. As before, bias was quantified using the error factor (equation (6)), so that it reflects the difference between the true average erosion rate and the erosion rate inferred from the 0.25–0.5 mm stream sediment alone. Because studies do not generally know a priori how sediment size varies across a catchment, we considered multiple scenarios spanning the range of altitudinal gradients in sediment size shown in Figure 4a. Likewise, we modeled a range of scenarios in which erosion rates increase with elevation. Thus, we were able to explore not only the effects of relief but also the effects of different altitudinal gradients in both sediment size and erosion rates.

For all combinations of nonzero gradients in erosion rate and sediment size, we found that the error factor is larger in the high-relief catchment (Figure 6). This is because the ranges in absolute sediment sizes and erosion rates are larger in the high-relief catchment for a given set of gradients. Therefore, in our simulations, the degree to which the upper elevations were underrepresented in the sampled sediment was always smaller in the low-relief catchment, because of its lower overall range in sediment sizes. Moreover, the cosmogenic nuclide concentrations that were underrepresented in the sample were not as different from the catchment average because of the narrower range in erosion rates of the low-relief catchment. Together these mitigating factors made the 0.25–0.5 mm sand much more representative of the average erosion rate in the low-relief catchment.

For both the high- and low-relief catchments, we found that there is no bias in the inferred average erosion rate when sediment size does not vary with altitude (Figure 6). Under this condition, equation (4) effectively reduces to equation (3) (such that the conventional formulation is valid) because $f_{0.25-0.5\text{mm}}$ is the same everywhere in the catchment. The 0.25–0.5 mm stream sediment therefore accurately reflects the catchment-average erosion rate. Such a condition should arise whenever $f_{0.25-0.5\text{mm}}$ is the same throughout the catchment, including scenarios in which the proportions of other size classes vary across the catchment. However, when $f_{0.25-0.5\text{mm}}$ varies with elevation, the error factor increases with increasing gradients in sediment size for all erosion rate scenarios in both catchments (Figure 6).

The sense of bias differs depending on how quickly erosion rates increase with elevation. When erosion rates are uniform or increase slowly with altitude (purple lines in Figure 6), the catchment-average erosion rate will be too large when only 0.25–0.5 mm sand is sampled and analyzed. This is because the underrepresented sediment from higher elevations has higher-than-average nuclide production rates and thus higher-than-average cosmogenic nuclide concentrations. The average cosmogenic nuclide concentration in the sample will be too low, and the inferred erosion rate will be too high. Conversely, when the altitudinal increase in erosion rates outpaces the increase in nuclide production rates (green lines in Figure 6), higher elevations will have lower-than-average nuclide concentrations and the sense of bias will be reversed: The average cosmogenic nuclide concentration in the sampled sand will be too high, and the inferred erosion rate will be too low.

The trade-off between increases in erosion rate and nuclide production rates can lead to a balance in which little to no bias arises even though sediment size increases across the catchment (gray curves in Figure 6). In these special cases, as altitude increases, the decrease in nuclide concentrations due to increasing erosion

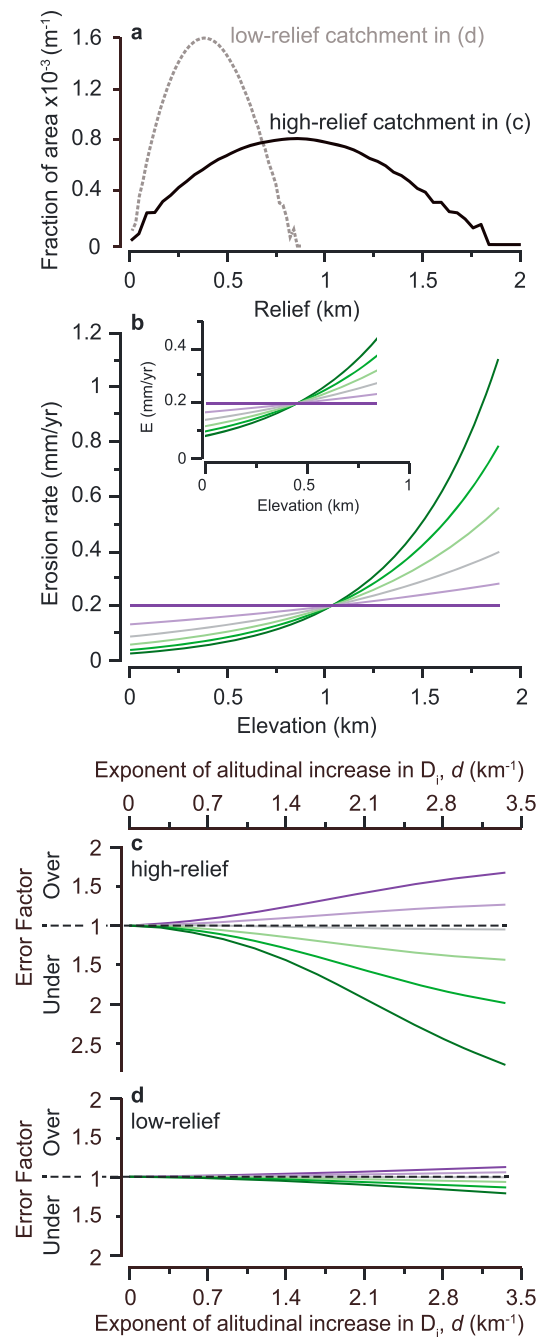


Figure 6. Forward modeling of bias as a function of spatial variations in erosion rate for two synthetic catchments with different relief. (a) Synthetic elevation distributions of the two catchments. (b) Modeled erosion rates vary from 0.002 to 1.1 mm/yr overall for the high-relief catchment but span a narrower range in the low-relief catchment (inset). (c and d) Sediment size increases with altitude according to exponential relationships with gradients corresponding to values on horizontal axes. Results from simulations on the high-relief catchment (Figure 6c) show that bias increases with increasing gradients in both sediment size and erosion rate. The catchment-averaged erosion rate may be overestimated or underestimated, depending on the steepness of the altitudinal gradient in erosion rate (see text). Results from the low-relief catchment (Figure 6d) show that the bias is much lower in all of our simulations due to the narrower range in erosion rates and median sediment sizes across the low relief catchment.

rates is roughly balanced by the increase in nuclide concentrations due to increasing nuclide production rates. Thus, cosmogenic nuclide concentrations are the same everywhere in the catchment. High elevations are still underrepresented in the sample due to the altitudinal gradient in sediment size, but no bias arises in the erosion rate estimate because of the spatial uniformity in nuclide concentrations.

Our analysis shows that both the magnitude and sense of bias are influenced by relief and altitudinal gradients in sediment size and erosion rate. For example, in the high-relief catchment in Figure 6c, the error factor can be as high as 3 when erosion rates increase from 0.002 to 1.1 mm/year and median sediment size increases from 1 to 700 mm from bottom to top across the catchment. This is a realistic range in erosion rates and sediment sizes for steep landscapes [e.g., Riebe *et al.*, 2015], implying that significant bias could be introduced in a wide range of catchments by sampling only the 0.25–0.5 mm sand. The bias is significantly lower for the low-relief synthetic catchment under the same altitudinal gradients in erosion rates and sediment sizes, because the overall range in erosion rates and median sediment sizes is much lower due to the lower relief (i.e., E_i spans 0.08–0.45 mm/yr and D_i spans 1–20 mm, respectively).

4.3. Effects of Difference in Area

Thus far, our analysis of variations in bias has focused on altitudinal gradients in erosion rate and sediment size as factors of interest. Next, we hold these gradients constant and explore the relative importance of variations in catchment relief and area. Our results in Figure 6 show that higher relief leads to more bias. To quantify the influence of area—and its importance relative to relief—we included the effects of breakdown (equations (7) and (8)) in our analysis. This approach

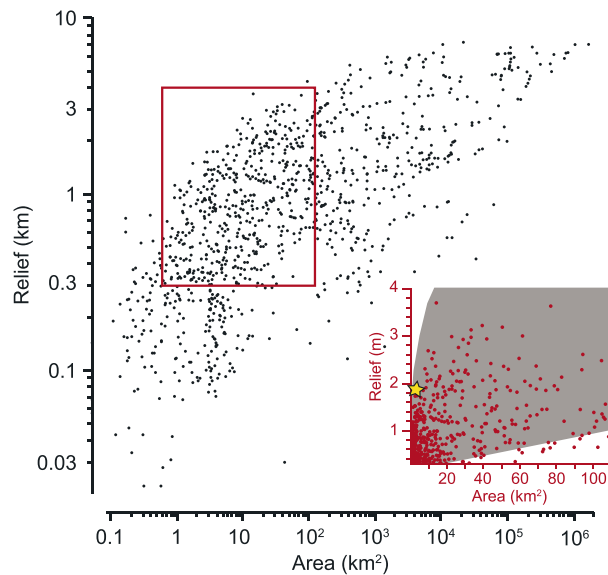


Figure 7. Area versus relief (note log axes) for catchments where ^{10}Be has been used to quantify catchment-average erosion rates (based on data compiled by Portenga and Bierman [2011]). Red box shows range spanned in inset (note linear axes; area axis starts at 0.6 km^2), which highlights the range of values considered in our analysis of the effects of area and relief on the magnitude of the grain size bias (gray box). Star marks the combination of catchment area and relief draining to the Inyo Creek sampling point (see Figure 3a).

catchments ($>110\text{ km}^2$) where complications due to the dynamics of floodplain deposition might dominate over the grain size bias. We imposed the same increase in sediment size ($D_i = D_{\min}e^{0.0017(Z_i - Z_0)}$) and erosion rate ($E_i = 0.01e^{0.0013(Z_i - Z_0)}$) across all combinations of catchment relief and area. These gradients yielded a maximum range in median sediment size from 1 to 1024 mm and erosion rates ranging from 0.01 to 1.8 mm/yr in the catchments with the highest relief. The ranges in sediment size and erosion rates are smaller for catchments with less relief. This retains consistency across all analyses without imposing unrealistic ranges in the high-relief catchments. One implication of this approach is that we cannot simulate the large spatial variations in erosion rate observed in places like Inyo Creek, where the modeled 0.01–0.13 mm/yr range is much lower than the 0.01–1.5 mm/yr range implied by apatite helium ages and cosmogenic nuclides in stream sediment. If we used model parameters that reproduced the observed range at Inyo Creek across all modeled catchments, the largest catchments would produce unrealistically large median sediment sizes ($D_i > 10\text{ m}$) at high elevations. Instead, we used the same smaller increases in erosion rate and sediment size for every modeled catchment; thus, we can identify combinations of area and relief that produce lead to relatively high and low bias.

To evaluate the effects of breakdown, we used three different breakdown coefficients: $\alpha = 0.0001$, $\alpha = 0.0002$, and $\alpha = 0.0003\text{ m}^{-1}$ in equations (7) and (8). In each case, we found that bias increases with relief for a given area (Figure 8). This is consistent with our analysis of Figure 6, where the bias arises because both sediment size and erosion rate increase with altitude, leading to an underrepresentation of the faster erosion rates in the higher-elevation portions of the catchment. As area increases, bias becomes more sensitive to relief (Figure 8) due to the longer travel distances and thus greater loss of mass by abrasion during transport of the sampled (0.25–0.5 mm) sediment. This is consistent with our analysis of Figure 4: breakdown amplifies bias by contributing to the underrepresentation of more distant, higher-elevation portions of the catchment in the sample. However, the increase in sensitivity is most pronounced at smaller areas, due to the exponential relationship between particle size and travel distance (equation (4)). As the intensity of breakdown increases (represented in increasing α), the sensitivity to area is amplified (Figure 8).

The bias shown in Figure 8 spans a relative scale, from high to low, because the magnitude and sense of grain size bias for a landscape will depend on site-specific factors, such as the spatial variation in sediment size and

helps more realistically define the range of natural landscapes that may be susceptible to significant bias and helps us explore the sensitivity of bias to both area and relief.

To vary both area and relief in our analysis, we modified the parameters in the scaling relationships as described in Appendix A. This created an array of synthetic catchments with different combinations of area and relief. We then incorporated the distributions of elevation and travel distance for each synthetic catchment into our forward sediment mixing model to quantify effects of both the variation in sediment production (equation (4)) and the effect of sediment breakdown during transport (equations (7) and (8)).

We considered a subset of the range in catchment area and relief spanned by previous cosmogenic nuclide studies (Figure 7), focusing on mountain landscapes with relief greater than 300 m (Figure 7b). We avoided large

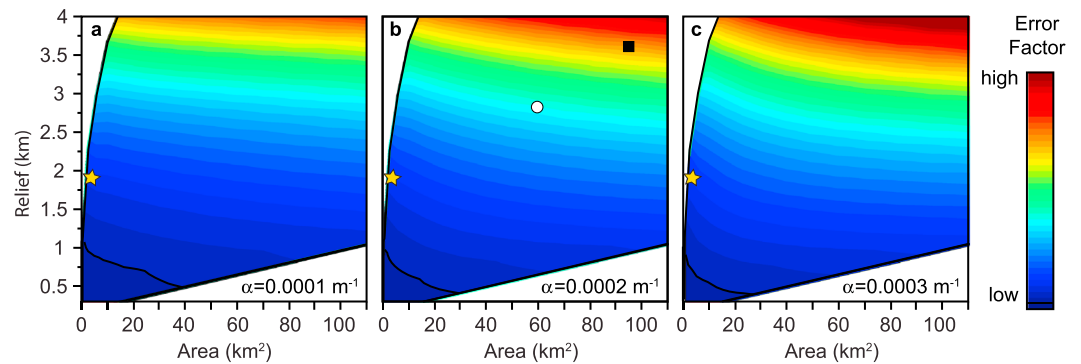


Figure 8. The influence of area and relief on the grain size bias for three different breakdown coefficients. Here erosion rates increase with altitude according to $E_i = 0.01e^{0.0013(Z_i - Z_0)}$ and sediment size increases with altitude according to $D_i = e^{0.00174(Z_i - Z_0)}$. Thick black line represents threshold between overestimating and underestimating erosion rates (i.e., where the error factor = 1). (a) When the breakdown coefficient is low, the bias is not strongly sensitive to area. (b) The sensitivity to area increases with increasing breakdown coefficient, reflecting an increasing underrepresentation of more distal points in the catchment due to increasing breakdown. (c) When the breakdown coefficient is high, breakdown becomes increasingly sensitive to relief with increasing area. To show how the relative scale of bias translates into absolute values, we highlight the area and relief at Inyo Creek (star), where the error factor is nearly 3 based on cosmogenic nuclides and detrital thermochronometry in multiple sediment sizes [Riebe et al., 2015], and two other catchments (white circle and black square)—see text.

erosion rate, which are generally unknown, a priori. To explore how the relative scaling in Figure 8 might translate to an absolute scaling of likely errors in the real world, we pose several hypothetical cases. For reference, the yellow star in each panel marks the area and relief of Inyo Creek, where erosion rates inferred from ^{10}Be in sand appear to underestimate the catchment-average erosion rate by a factor of roughly three [Riebe et al., 2015]. In comparison, the white circle in Figure 8b marks a catchment with relief = 2.8 km and area = 60 km²; the bias is 1.9 times larger here than at a catchment with Inyo Creek's area and relief under the same breakdown rate and the same altitudinal increase in sediment size and erosion rate. Similarly, at the black square, representing a catchment with area = 95 km² and relief = 3.6 km, the estimated bias is 3.0 times higher than the bias at the Inyo Creek reference catchment.

5. Discussion

Our analysis of bias across gradients in sediment size, erosion rates, catchment area, and relief revealed the following general patterns: The bias can be bigger than a factor of 3, based on our analysis of Inyo Creek and our modeling of larger self-similar catchments. Steeper altitudinal gradients in sediment size lead to larger bias, all else equal. Bias also increases with increasing altitudinal gradients in erosion rates when sediment size changes with altitude. However, if sediment size does not vary across the catchment, variations in erosion rates are captured in the catchment-wide average from any sediment size in the channel, as assumed in the formulation of equation (3) [Brown et al., 1995; Bierman and Steig, 1996; Granger et al., 1996]. When sediment size increases with altitude, higher relief and area both lead to higher bias. The effects of relief dominate over the effects of area. The sensitivity of bias to area is higher when area is relatively small and when the intensity of breakdown is high (Figure 8). Overall, we found that larger, higher-relief catchments are more susceptible to bias.

Our analysis demonstrates that the grain size bias can be significantly larger than the 8–10% errors introduced by the combination of analytical error, uncertainty in production rates, and uncertainty in shielding by topography and snow [e.g., Dunai, 2010]. They are similar in magnitude to errors introduced by failing to account for factors such as chemical enrichment of quartz, glaciation, and poor sediment mixing. For example, ignoring mass loss due to chemical weathering neglects the associated increase in quartz residence times and thus may introduce factor-of-2 underestimates of ^{10}Be -inferred erosion rates in catchments with intensively weathered soils [Riebe and Granger, 2013]. Conversely, ignoring shielding by ice can lead to factor-of-3 overestimates in erosion rates for catchments that have been covered by glaciers [Glotzbach et al., 2013]. Meanwhile, insufficient mixing of sediment from tributaries can introduce factor-of-2 errors in

either direction [Binnie *et al.*, 2006], and episodic delivery of depth-shielded sediment by landslides may introduce even larger errors in small catchments [Yanites *et al.*, 2009]. Grain size bias can be as large as or larger than many of these sources of error and thus warrants careful consideration in study design.

5.1. Limitations of our Analysis

Although our simulations capture variations in sediment size across slopes, they do not account for the potential for error due to erosion of sediment from depths that are shielded from cosmic rays. If sediment size varies with depth below the landscape surface, different grain sizes could have different cosmogenic nuclide concentrations due to the exponential decrease in cosmogenic nuclide production with depth. The potential for this type of bias was highlighted in the earliest study of catchment-average erosion rates from cosmogenic nuclides [Brown *et al.*, 1995]; lower cosmogenic nuclide concentrations in coarser stream sediment sizes were attributed to delivery of the sediment from greater depths on catchment slopes by landsliding. Our model could be adapted to account for this complication. However, our goal here was to explore the bias that arises due to lateral rather than vertical variations in sediment size distributions, without the confounding effects of other factors. Thus, our analysis does not account for potential variations in sediment size with depth.

Although our analysis explicitly incorporates spatial variations in long-term erosion rates, it does not account for the stochastic delivery of packets of sediment from isolated areas within the catchment by landsliding [Benda and Dunne, 1997; Binnie *et al.*, 2007]. Rather, our approach assumes that stream sediment is eroded from all areas and mixed in the stream according to the spatial distribution of long-term average erosion rates. Previous studies have demonstrated that complications from landslides will be an important additional factor to consider in the steep mountain catchments where grain size bias is likely to arise [Niemi *et al.*, 2005; Reinhardt *et al.*, 2007; Yanites *et al.*, 2009]. Because our model is spatially explicit, it could be adapted to incorporate stochastic erosion from landsliding. However, this is beyond the scope of this study.

Our model could also be adapted to incorporate the effects of variations in lithology across the study catchments. Spatial variability in bedrock lithology could influence nuclide concentrations in stream sediment in at least two ways. First, differences in concentration of the host mineral (usually quartz) across the catchment could lead to underrepresentation or overrepresentation of some parts of the landscape in the sampled stream sediment [Granger and Riebe, 2014; Carretier *et al.*, 2015]. For instance, if bedrock exposed at upper elevations is quartz-poor relative to bedrock at lower elevations, upper elevations will contribute less quartz than lower elevations, even if erosion rates are spatially uniform. Thus, the upper elevations, which have faster production rates of cosmogenic nuclides, would be underrepresented in the sample, and the estimated erosion rate would be too high. The resulting lithologic bias resembles the grain size bias in that it arises because some elevations are underrepresented in the sample. With a priori knowledge of bedrock lithology and mineralogy, the analysis of bias presented here could be modified to incorporate spatial variations in host mineral concentration by introducing it as an additional term in equation (4), thus accounting for the relative fraction of the host mineral contributed from different parts of the landscape. In our simulations, we assumed that host mineral concentrations were uniform across each catchment.

In addition to introducing differences in host mineral concentrations, lithologic differences in weathering rates and styles could also lead to spatial variations in the sizes of sediment produced on slopes. This could lead to differences in cosmogenic nuclide concentrations across stream sediment sizes. For instance, sandstone will tend to produce sand-sized particles, whereas a pebble conglomerate in the same catchment will tend to produce pebbles, sand, and smaller particles. If the sandstone and conglomerate are exposed at different elevations or are eroding at different rates, pebbles and sand in the stream sediment would harbor different cosmogenic nuclide concentrations due to differences in nuclide production rates or hillslope erosion rates. Similar differences could arise due to variations in fracture density, igneous texture (e.g., fine grained versus pegmatitic), and other intrinsic differences in bedrock that control the size of sediment produced on hillslopes. To account for variations in lithology, the forward model could be modified to include changes in sediment size or erosion rate across lithologic contacts.

In our analysis of bias, we assumed that changes in sediment size and erosion rates are continuous with elevation, which is consistent with the climatic control on sediment production that has been observed in previous studies [Marshall and Sklar, 2012; Riebe *et al.*, 2015]. Because we used continuous functions, our approach is best suited to capturing the trends rather than the details in the relationships between climate,

sediment size, and erosion rate. In practice, the altitudinal increases in sediment size and erosion rates may be more complex than the simple exponential functions used here. Our forward model is spatially explicit and is therefore capable of handling such complexities, but we refrained from adding them here because they are poorly understood. Likewise, we used a simple exponential function to describe reduction of sediment size by abrasion (equation (7)), recognizing that large uncertainties remain in predicting sediment breakdown in natural systems [Sklar *et al.*, 2006]. Additional complexity might be needed to account for the fact that particles are reduced in size not only by abrasion during transport but also by fracturing [Attal and Lavé, 2009; Chatanantavet *et al.*, 2010; Le Bouteiller *et al.*, 2011]. Moreover, our implicit assumption that size reduction occurs at the same fractional rate for each size class, from boulders to sand, is likely an oversimplification. As more is learned about how particle sizes are reduced during transport, the behavior could be incorporated into our forward model.

5.2. Implications of Ignoring Grain Size Bias

Our results indicate that significant bias can arise in studies that fail to sample sediment that is representative of catchment-wide erosion rates. In many instances, the bias may be safe to ignore because the catchment is small and sediment size does not vary by much across it. For example, in the Fort Sage Mountains of California, where results from equation (3) compare well with independent measurements of erosion rates from two catchments, cosmogenic ^{10}Be differ by less than 50% across sediment sizes in catchment streams [Granger *et al.*, 1996]. This may reflect both the relatively low relief (400 m) of the Fort Sage Mountain catchments and the tendency of bedrock to produce grus of relatively uniform size across hillslopes. Under such conditions, there is little cause for concern regarding interpretations of cosmogenic nuclides in stream sediment.

In contrast, our results indicate that bias may be important to consider in landscapes that have higher relief and either large area or a propensity for spatial variations in sediment size. In such landscapes, bias may be substantial and may vary systematically with factors of interest such as climate and relief. This raises the possibility of artifactual correlations in previous cosmogenic nuclide studies of erosion rates. For example, when sediment size and erosion rate both increase with elevation, the correlation between bias and catchment relief (Figure 8) would lead to substantial underestimation of the correlation between average erosion rates and catchment relief. This suggests that previous studies may have underestimated the role of relief in explaining variations in catchment-wide erosion rates. More generally, artifactual correlations due to grain size bias may help explain why it has been difficult to detect expected trends in catchment-wide erosion rates across relief and climate [Riebe *et al.*, 2000, 2001a; von Blanckenburg, 2005].

5.3. Accounting for Grain Size Bias

Understanding variations in the sizes of sediment produced by erosion across hillslopes remains a fundamental challenge in geomorphology. Because little is known about how sediment size varies across mountain slopes, it is difficult to know a priori whether grain size bias may be large enough to influence interpretations of cosmogenic nuclides in sediment. This makes it difficult to identify catchments where the traditional approach of sampling a narrow range of sediment sizes is appropriate. However, evidence suggests that sediment size can vary markedly with climate and topography [Marshall and Sklar, 2012; Riebe *et al.*, 2015; Attal *et al.*, 2015], implying that the bias may need to be accounted for in many landscapes.

In catchments where many sediment sizes are present in the stream, bias can be detected using thermochronometric and cosmogenic nuclide data from multiple sediment sizes. If thermochronometric ages vary among sizes, it may indicate that the sizes originate from different elevations [Vermeesch, 2007] and thus that the size distributions of eroded sediment vary with elevation [Riebe *et al.*, 2015]. Likewise, if cosmogenic nuclide concentrations vary with sediment sizes in the stream, it may indicate that the sizes originate from locations with different erosion rates [Belmont *et al.*, 2007; Codilean *et al.*, 2014; Attal *et al.*, 2015], which would also indicate that sediment size varies across catchment slopes.

In practice, there will be many scenarios in which neither thermochronometry nor cosmogenic nuclides alone will unequivocally reveal the potential for grain size bias in catchment-average erosion rates. For example, many catchments lack datable minerals or systematic age-elevation relationships for thermochronometric fingerprinting of sediment source elevations. Meanwhile, cosmogenic nuclides can vary with sediment size due to other complications besides a grain size bias [Matmon *et al.*, 2003; Belmont *et al.*, 2007; Codilean

et al., 2010, 2014; *Puchol et al.*, 2014; *Aguilar et al.*, 2014; *Attal et al.*, 2015], making interpretations of data from multiple sediment sizes inherently equivocal. For instance, variations in ^{10}Be concentrations with sediment sizes could reflect the preferential breakdown of coarse particles originating from higher elevations, where nuclide production rates are higher [*Matmon et al.*, 2003]: This may help explain why coarse clasts have relatively low cosmogenic nuclide concentrations in some streams [*Matmon et al.*, 2003; *Belmont et al.*, 2007]. Such an effect could be simulated in our forward model by making coarser sizes more prone to breakdown than finer sizes (i.e., such that α increases with D). But that would fail to address the alternative possibility that relatively low ^{10}Be concentrations in coarser sediment reflect preferential delivery of cosmic-ray-shielded coarse particles from deep-seated landslides [*Belmont et al.*, 2007; *Brown et al.*, 1995]. The influence of these mechanisms could be deciphered using a combination of thermochronometry and cosmogenic nuclides in multiple sediment sizes, but both techniques would need to be applicable at the catchment in question.

If thermochronometry is impossible and cosmogenic nuclides are equivocal on their source of variation, the potential for bias could nonetheless be evaluated in a catchment using more conventional geomorphological observations. In particular, direct measurements of the sizes of sediment produced on hillslopes across the catchment could prove invaluable. Inferences from remote sensing, satellite photos, and known climatic variability across the catchment might also be helpful. For example, if remotely sensed vegetation is less common in some places than others, it may indicate that there are differences in geomorphic processes that have led to variations in sediment size [*Riebe et al.*, 2015]. Likewise, if satellite photos show that talus aprons are more common at higher elevations, it might indicate that grain size increases with elevation. Similarly, if climate data suggest that altitudinal variations in frost cracking are significant across the catchment [*Hales and Roering*, 2007], it could be indicative of altitudinal differences in sediment sizes on slopes [*Riebe et al.*, 2015]. We suggest that researchers should use all of the available information to evaluate how sediment size might vary across the landscape when developing sampling strategies for any stream that carries a wide range of sediment sizes.

If available information suggests that grain size varies across catchment slopes, then it may be possible to quantify and account for the resulting grain size bias by analyzing multiple sediment sizes for cosmogenic nuclides. However, more work is needed to validate this idea. It may even be possible to quantify how grain size distributions vary across slopes by combining detrital thermochronometry and cosmogenic nuclide measurements from multiple sediment sizes in the stream [*Riebe et al.*, 2015]. Cosmogenic nuclides reflect the pace of erosion on slopes where sediment is produced, whereas thermochronometric ages identify the source elevations of individual sediment grains. This means that rather than specifying altitudinal variations in erosion rates and sediment sizes in a forward model (as we have done here to explore bias), one could instead quantify these variations in an inverse approach using observations from sediment in the stream. For example, at Inyo Creek, a coupled analysis of cosmogenic nuclides and thermochronometric ages in two sediment sizes has shown that both the erosion rate and the size of sediment produced on slopes increase markedly with altitude [*Riebe et al.*, 2015]. With measurements from additional stream sediment sizes, it should be possible to more precisely quantify the relationships between altitude, sediment size, and erosion rate in catchments.

6. Conclusions

Here we identified a previously underappreciated but potentially widespread bias in cosmogenic nuclide studies of catchment-average erosion rates. This bias arises in studies that sample a narrow range of stream sediment sizes (e.g., sand) from catchments where gradients in weathering lead to spatial variability in the sizes of sediment produced on slopes. The grain size bias increases with catchment relief and area and is most pronounced in catchments with steep altitudinal gradients in sediment size and erosion rates, leading to errors of a factor of 3 or more. Erosion rates may be overestimated or underestimated, depending on how erosion rates vary across the catchment. When erosion rates increase quickly with altitude, the bias leads to an underestimate of the catchment-average erosion rate. Conversely, if erosion rates increase slowly or decrease with altitude, the bias leads to an overestimate of catchment-average erosion rate. Sediment breakdown during transport increases the bias, regardless of how erosion rates vary across the catchment.

Modeling results presented here provide a theoretical basis for identifying landscapes where cosmogenic nuclides could substantially overestimate or underestimate catchment-average erosion rates. Data from

Inyo Creek demonstrate that such biases can be quantified using cosmogenic nuclides and detrital thermochronometry in multiple sediment sizes. When combined together, these measurements may also provide a way to study spatial variations in sediment production and erosion and thus move beyond the catchment averages of conventional cosmogenic nuclide studies. By quantifying details of how erosion and weathering vary across catchments, such work promises to provide new insights into the feedbacks between erosion, climate, topography, and tectonics.

Appendix A: Generating Synthetic Distributions of Elevation and Travel Distance

To build synthetic distributions of elevation and travel distance following the approach of *Sklar et al.* [2016], we needed three things: an expression for the longitudinal channel profile, an expression for the longitudinal ridge profile, and a way to distribute catchment area between the two profiles. To create a channel profile, we combined two common power-law scaling relationships. The first is Flint's Law, which relates channel slope (S) and upstream drainage area (A) [Flint, 1974]:

$$S = k_s A^{-\theta}. \quad (\text{A1})$$

Here k_s and θ are empirical constants. The second is Hack's Law (equation (A2)) which describes the scaling between distance along the stream and drainage area [Hack, 1957; Rigon et al., 1996] and can be written in terms of the local distance upstream of the catchment outlet (x):

$$A = k_A (L_{\max} - x)^H, \quad (\text{A2})$$

where k_A and H are empirical constants. Here L_{\max} is defined as the longest travel distance to the catchment outlet, measured along the stream channel.

Combining equations (A1) and (A2) yields an expression for the slope of the channel as a function of distance upstream, which we then integrate to obtain the elevation of the channel (z_c) as a function of upstream travel distance, x :

$$z_c = k_c \left[L_{\max}^{1-\theta H} - (L_{\max} - x)^{1-\theta H} \right]. \quad (\text{A3})$$

Here k_c is a coefficient calculated as follows:

$$k_c = \frac{k_s k_A^{-\theta}}{1 - \theta H}. \quad (\text{A4})$$

Equation (A3) describes the channel profile for the fluvial part of the landscape [e.g., Whipple and Tucker, 1999].

At travel distances on the long profile that fall above the fluvial part of the landscape, this relationship may not hold [e.g., Stock and Dietrich, 2003]. To approximate the channel slope in these reaches, we used a constant slope (S_h) defined by the coefficients from equations (A1) and (A2) according to equation (A5).

$$S_h = \frac{k_s}{k_A^\theta} (L_{\max} - x)^{-\theta H}. \quad (\text{A5})$$

This slope extends from the "channel head," at L_{ch} , to the catchment divide, at L_{\max} . Equations (A3) and (A5) can be used to calculate the elevation of the unchanneled valley above the channel head according to equation (A6).

$$z_c = k_c (L_{\max}^{1-\theta H} - L_{\text{ch}}^{1-\theta H}) + S_h (x - x_{\text{ch}}). \quad (\text{A6})$$

Here x_{ch} is the distance measured along the channel between the catchment divide and the channel head.

Together, equations (A4) and (A6) define the longitudinal channel profile from catchment mouth to its divide. Equation (A4) applies when $x < x_{\text{ch}}$; equation (A6) applies when x lies between x_{ch} and the divide (i.e., L_{\max}). The elevation of the channel profile at the maximum travel distance, $z_{c_{\max}}$, can be calculated from equation (A7).

$$z_{c_{\max}} = k_c (L_{\max}^{1-\theta H} - L_{\text{ch}}) + S_h L_{\text{ch}}. \quad (\text{A7})$$

Table A1. Parameters Used to Generate Synthetic Distributions of Elevation and Travel Distance

Parameter	Value Used or Range Explored	Description
k_s	5–25	Intercept coefficient for channel profile
k_A	1.28	Hack's Law coefficient
L_{\max}	600–20,000 m	Longest travel distance
θ	0.31	Channel curvature coefficient
H	1.75	Hack's Law exponent
L_{ch}	600 m	Distance from catchment divide to channel head
k_{Re}	0.6	Ridge profile coefficient
β_1	2.6	First shape parameter in beta distribution
β_2	3.4	Second shape parameter in beta distribution

To generate a synthetic ridge profile, we used a power law to describe the relationship between elevation and distance, where z_R is the elevation of the ridge as a function of upstream travel distance (x) and k_{Re} is an adjustable parameter.

$$z_R = k_{\text{Re}}x^P. \tag{A8}$$

The exponent P depends on the parameters used in the channel profile. If the channel and ridge profiles meet at both the ridge, where $x = L_{\max}$, and the channel outlet, where $x = 0$, we can solve for P , as follows:

$$P = \frac{\log\left(\frac{z_{\text{cmax}}}{k_{\text{Re}}}\right)}{\log(L_{\max})}. \tag{A9}$$

Overall, the equations used to build longitudinal channel and ridge profiles include seven parameters that can be tuned to change the size and shape of the synthetic catchment they define.

The next step in building synthetic distributions of elevation and travel distance is to distribute catchment area in a realistic way between the channel and ridge profiles. The elevations of the highest ridge and lowest channel in each travel distance bin define the top and bottom of the area distribution at the travel distance. To assign area within that range of elevations, we used a beta distribution. The beta distribution is defined by two shape parameters, β_1 and β_2 . To define a realistic β_1 and β_2 for our simulations, we used best fit values derived from a chi-square minimization analysis of the observed distribution of area at each travel distance in the Inyo Creek catchment. The best fit values of β_1 and β_2 were 2.6 and 3.4, respectively.

We tuned parameters in equations (A1)–(A9) by eye for a good fit to the DEM from Inyo Creek, which we binned into increments of 40 m for elevation and 100 m for travel distance. The best fit parameters fall within the range of published values for steep channels [e.g., Hack, 1957; Whipple and Tucker, 1999; Tucker and Whipple, 2002] and are reported in Table A1.

Together, the parameters in Table A1 can be used to generate synthetic distributions of elevation and travel distance, for comparison with the hypsometry and width function of Inyo Creek. The agreement between the synthetic and observed distributions (Figure 5) suggests that the approach outlined in this appendix can be used to produce realistic inputs for our forward model of sediment erosion and mixing.

To explore the effects of varying catchment relief and area on the grain size bias, we generated synthetic distributions of elevation and travel distance that are self-similar to those at Inyo Creek by varying two parameters: the longest travel distance (L_{\max}) and the channel profile intercept (k_s). All other parameters remained the same for the simulation results displayed in Figure 8. This approach allowed us to isolate the effects of catchment area and relief on the grain size bias, without the potentially confounding effects of changes the catchment shape. To generate the plots in Figure 8, we explored a range in L_{\max} from 600 to 20,000 m and a range in k_s from 5 to 25. This produced a range in catchment area between 0.5 and 110 km² and a range in catchment relief from 300 to over 6000 m. Catchment relief in natural landscapes rarely exceeds 4000 m within the range of areas considered; thus, we plot catchment relief of 4000 m or less to maintain realistic ranges of catchment area and relief. We also explored the influence of catchment shape (by varying θ and k_{Re}) but found it to have a much smaller effect on the bias than either area or relief.

Acknowledgments

Model parameters can be found in the text, figures, and appendix. Data from Inyo Creek can be found in the references. This work was supported by National Science Foundation grants EAR 1325033 and EAR 1331939, a Geological Society of America graduate student research grant, a Wyoming NASA Space Grant, the Doris and David Dawdy Fund for Hydrologic Research, and the Ann and Gordon Getty Foundation. The authors declare no conflict of interest.

References

- Abbühl, L. M., K. P. Norton, F. Schlunegger, O. Kracht, A. Aldahan, and G. Possnert (2010), El Niño forcing on ^{10}Be -based surface denudation rates in the northwestern Peruvian Andes? *Geomorphology*, *123*(3–4), 257–268, doi:10.1016/j.geomorph.2010.07.017.
- Aguilar, G., S. Carretier, V. Regard, R. Vassallo, R. Riquelme, and J. Martinod (2014), Grain size-dependent ^{10}Be concentrations in alluvial stream sediment of the Huasco Valley, a semi-arid Andes region, *Quat. Geochronol.*, *19*, 163–172, doi:10.1016/j.quageo.2013.01.011.
- Attal, M., and J. Lavé (2006), Changes of bedload characteristics along the Marsyandi River (central Nepal): Implications for understanding hillslope sediment supply, sediment load evolution along fluvial networks, and denudation in active orogenic belts, in *Tectonics, Climate, and Landscape Evolution*, *Geol. Soc. Am. Spec. Pap.*, vol. 398, pp. 143–171.
- Attal, M., and J. Lavé (2009), Pebble abrasion during fluvial transport: Experimental results and implications for the evolution of the sediment load along rivers, *J. Geophys. Res.*, *114*, F04023, doi:10.1029/2009JF001328.
- Attal, M., S. M. Mudd, M. D. Hurst, B. Weinman, K. Yoo, and M. Naylor (2015), Impact of change in erosion rate and landscape steepness on hillslope and fluvial sediments grain size in the Feather River basin (Sierra Nevada, California), *Earth Surf. Dyn.*, *3*, 201–222.
- Belmont, P., F. J. Pazzaglia, and J. C. Gosse (2007), Cosmogenic ^{10}Be as a tracer for hillslope and channel sediment dynamics in the Clearwater River, western Washington State, *Earth Planet. Sci. Lett.*, *264*(1–2), 123–135, doi:10.1016/j.epsl.2007.09.013.
- Benda, L., and T. Dunne (1997), Stochastic forcing of sediment supply to channel networks from landsliding and debris flow, *Water Resour. Res.*, *33*(12), 2849–2863, doi:10.1029/97WR02388.
- Bierman, P., and E. J. Steig (1996), Estimating rates of denudation using cosmogenic isotope abundances in sediment, *Earth Surf. Processes Landforms*, *21*(2), 125–139.
- Bierman, P. R., and M. Caffee (2001), Slow rates of rock surface erosion and sediment production across the Namib Desert and escarpment, southern Africa, *Am. J. Sci.*, *301*(4–5), 326–358, doi:10.2475/ajs.301.4-5.326.
- Bierman, P. R., K. A. Marsella, C. Patterson, P. T. Davis, and M. Caffee (1999), Mid-Pleistocene cosmogenic minimum-age limits for pre-Wisconsinan glacial surfaces in southwestern Minnesota and southern Baffin Island: A multiple nuclide approach, *Geomorphology*, *27*(1–2), 25–39, doi:10.1016/S0169-555X(98)00088-9.
- Bierman, P. R., R. Coppersmith, K. Hanson, J. Neveling, E. W. Portenga, and D. H. Rood (2014), A cosmogenic view of erosion, relief generation, and the age of faulting in southern Africa, *GSA Today*, *24*(9), 4–11, doi:10.1130/GSATG206A.1.
- Binnie, S. A., W. M. Phillips, M. A. Summerfield, and L. Keith Fifield (2006), Sediment mixing and basin-wide cosmogenic nuclide analysis in rapidly eroding mountainous environments, *Quat. Geochronol.*, *1*(1), 4–14, doi:10.1016/j.quageo.2006.06.013.
- Binnie, S. A., W. M. Phillips, M. A. Summerfield, and L. K. Fifield (2007), Tectonic uplift, threshold hillslopes, and denudation rates in a developing mountain range, *Geology*, *35*(8), 743–746.
- Brown, E. T., R. F. Stallard, M. C. Larsen, G. M. Raisbeck, and F. Yiou (1995), Denudation rates determined from the accumulation of in situ-produced ^{10}Be in the Luquillo experimental forest, Puerto Rico, *Earth Planet. Sci. Lett.*, *129*(1–4), 193–202, doi:10.1016/0012-821X(94)00249-X.
- Carretier, S., V. Regard, and C. Soual (2009), Theoretical cosmogenic nuclide concentration in river bed load clasts: Does it depend on clast size? *Quat. Geochronol.*, *4*(2), 108–123, doi:10.1016/j.quageo.2008.11.004.
- Carretier, S., V. Regard, R. Vassallo, J. Martinod, F. Christophoul, E. Gayer, L. Audin, and C. Lagane (2015), A note on ^{10}Be -derived mean erosion rates in catchments with heterogeneous lithology: Examples from the western Central Andes, *Earth Surf. Processes Landforms*, *40*(13), 1719–1729, doi:10.1002/esp.3748.
- Casagli, N., L. Ermini, and G. Rosati (2003), Determining grain size distribution of the material composing landslide dams in the Northern Apennines: Sampling and processing methods, *Eng. Geol.*, *69*(1–2), 83–97, doi:10.1016/S0013-7952(02)00249-1.
- Chadwick, O. A., J. J. Roering, A. M. Heimsath, S. R. Levick, G. P. Asner, and L. Khomo (2013), Shaping post-orogenic landscapes by climate and chemical weathering, *Geology*, *41*(11), 1171–1174, doi:10.1130/G34721.1.
- Chatanantavet, P., E. Lajeunesse, G. Parker, L. Malverti, and P. Meunier (2010), Physically based model of downstream fining in bedrock streams with lateral input, *Water Resour. Res.*, *46*, W02518, doi:10.1029/2008WR007208.
- Clapp, E. M., P. R. Bierman, A. P. Schick, J. Lekach, Y. Enzel, and M. Caffee (2000), Sediment yield exceeds sediment production in arid region drainage basins, *Geology*, *28*(11), 995–998, doi:10.1130/0091-7613(2000)28<995:SYESPI>2.0.CO;2.
- Clapp, E. M., P. R. Bierman, and M. Caffee (2002), Using ^{10}Be and ^{26}Al to determine sediment generation rates and identify sediment source areas in an arid region drainage basin, *Geomorphology*, *45*(1–2), 89–104, doi:10.1016/S0169-555X(01)00191-X.
- Codilean, A. T., P. Bishop, T. B. Hoey, F. M. Stuart, and D. Fabel (2010), Cosmogenic ^{21}Ne analysis of individual detrital grains: Opportunities and limitations, *Earth Surf. Processes Landforms*, *35*(1), 16–27, doi:10.1002/esp.1815.
- Codilean, A. T., C. R. Fenton, D. Fabel, P. Bishop, and S. Xu (2014), Discordance between cosmogenic nuclide concentrations in amalgamated sands and individual fluvial pebbles in an arid zone catchment, *Quat. Geochronol.*, *19*, 173–180, doi:10.1016/j.quageo.2012.04.007.
- Cyr, A. J., and D. E. Granger (2008), Dynamic equilibrium among erosion, river incision, and coastal uplift in the northern and central Apennines, Italy, *Geology*, *36*(2), 103–106, doi:10.1130/G24003A.1.
- DiBiase, R. A., K. X. Whipple, A. M. Heimsath, and W. B. Ouimet (2010), Landscape form and millennial erosion rates in the San Gabriel Mountains, CA, *Earth Planet. Sci. Lett.*, *289*(1–2), 134–144, doi:10.1016/j.epsl.2009.10.036.
- DiBiase, R. A., A. M. Heimsath, and K. X. Whipple (2012), Hillslope response to tectonic forcing in threshold landscapes: Threshold hillslope response to tectonic forcing, *Earth Surf. Processes Landforms*, *37*(8), 855–865, doi:10.1002/esp.3205.
- Dietrich, W. E., R. Reiss, M.-L. Hsu, and D. R. Montgomery (1995), A process-based model for colluvial soil depth and shallow landsliding using digital elevation data, *Hydrol. Processes*, *9*(3–4), 383–400, doi:10.1002/hyp.3360090311.
- Drever, J. I., and J. Zobrist (1992), Chemical weathering of silicate rocks as a function of elevation in the southern Swiss Alps, *Geochim. Cosmochim. Acta*, *56*(8), 3209–3216, doi:10.1016/0016-7037(92)90298-W.
- Ferrier, K. L., C. S. Riebe, and W. H. Hahm (2016), Testing for supply-limited and kintec-limited chemical erosion in field measurements of regolith production and chemical depletion, *Geochem. Geophys. Geosyst.*, doi:10.1002/2016GC21021.
- Dunai, T. J. (2010), *Cosmogenic Nuclides: Principles, Concepts and Applications in the Earth Surface Sciences*, Cambridge Univ. Press, Cambridge, U. K.
- Flint, J. J. (1974), Stream gradient as a function of order, magnitude, and discharge, *Water Resour. Res.*, *10*(5), 969–973, doi:10.1029/WR010i005p0969.
- Fuchs, M. C., R. Gloaguen, S. Merchel, E. Pohl, V. A. Sulaymonova, C. Andermann, and G. Rugel (2015), Denudation rates across the Pamir based on ^{10}Be concentrations in fluvial sediments: Dominance of topographic over climatic factors, *Earth Surf. Dyn.*, *3*, 423–439, doi:10.5194/esurf-3-423-2015.
- Gabet, E. J. (2000), Gopher bioturbation: Field evidence for non-linear hillslope diffusion, *Earth Surf. Processes Landforms*, *25*(13), 1419–1428.
- Gasparini, N. M., G. E. Tucker, and R. L. Bras (1999), Downstream fining through selective particle sorting in an equilibrium drainage network, *Geology*, *27*(12), 1079–1082, doi:10.1130/0091-7613(1999)027<1079:DFTSPS>2.3.CO;2.

- Glotzbach, C., P. van der Beek, J. Carcaillet, and R. Delunel (2013), Deciphering the driving forces of erosion rates on millennial to million-year timescales in glacially impacted landscapes: An example from the Western Alps, *J. Geophys. Res. Earth Surf.*, *118*, 1491–1515, doi:10.1002/jgrf.20107.
- Granger, D. E., and C. S. Riebe (2014), 7.12—Cosmogenic nuclides in weathering and erosion, in *Treatise on Geochemistry*, 2nd ed., edited by H. D. H. K. Turekian, pp. 401–436, Elsevier, Oxford.
- Granger, D. E., J. W. Kirchner, and R. Finkel (1996), Spatially averaged long-term erosion rates measured from in situ-produced cosmogenic nuclides in alluvial sediment, *J. Geol.*, *104*(3), 249–257.
- Hack, J. T. (1957), Studies of longitudinal stream profiles in Virginia and Maryland, *U.S. Geol. Surv. Prof. Pap.* 294-B, 45–97.
- Hahn, W. J., C. S. Riebe, C. E. Lukens, and S. Araki (2014), Bedrock composition regulates mountain ecosystems and landscape evolution, *Proc. Natl. Acad. Sci. U.S.A.*, *111*(9), 3338–3343, doi:10.1073/pnas.1315667111.
- Hales, T. C., and J. J. Roering (2007), Climatic controls on frost cracking and implications for the evolution of bedrock landscapes, *J. Geophys. Res.*, *112*, F02033, doi:10.1029/2006JF000616.
- Heimsath, A. M., J. Chappell, W. E. Dietrich, K. Nishiizumi, and R. C. Finkel (2001), Late Quaternary erosion in southeastern Australia: A field example using cosmogenic nuclides, *Quat. Int.*, *83–85*, 169–185, doi:10.1016/S1040-6182(01)00038-6.
- Heimsath, A. M., J. Chappell, and K. Fifield (2010), Eroding Australia: Rates and processes from Bega Valley to Arnhem land, *Geol. Soc. London, Spec. Publ.*, *346*(1), 225–241.
- House, M. A., B. P. Wernicke, K. A. Farley, and T. A. Dumitru (1997), Cenozoic thermal evolution of the central Sierra Nevada, California, from (U-Th)/He thermochronometry, *Earth Planet. Sci. Lett.*, *151*(3–4), 167–179, doi:10.1016/S0012-821X(97)81846-8.
- Hurst, M. D., S. M. Mudd, M. Attal, and G. Hilley (2013), Hillslopes record the growth and decay of landscapes, *Science*, *341*(6148), 868–871, doi:10.1126/science.1241791.
- Kirchner, J. W., R. C. Finkel, C. S. Riebe, D. E. Granger, J. L. Clayton, J. G. King, and W. F. Megahan (2001), Mountain erosion over 10 yr, 10 k.y., and 10 m.y. time scales, *Geology*, *29*(7), 591–594, doi:10.1130/0091-7613(2001)029<0591:MEQYKY>2.0.CO;2.
- Kodama, Y. (1994), Experimental study of abrasion and its role in producing downstream fining in gravel-bed rivers, *J. Sediment. Res.*, *64*(1), 76–85.
- Krumbein, W. C. (1941), The effects of abrasion on the size, shape and roundness of rock fragments, *J. Geol.*, 482–520.
- Lal, D. (1991), Cosmic ray labeling of erosion surfaces: In situ nuclide production rates and erosion models, *Earth Planet. Sci. Lett.*, *104*(2), 424–439, doi:10.1016/0012-821X(91)90220-C.
- Le Bouteiller, C., F. Naaim-Bouvet, N. Mathys, and J. Lavé (2011), A new framework for modeling sediment fining during transport with fragmentation and abrasion, *J. Geophys. Res.*, *116*, F03002, doi:10.1029/2010JF001926.
- Lewin, J., and P. A. Brewer (2002), Laboratory simulation of clast abrasion, *Earth Surf. Processes Landforms*, *27*(2), 145–164, doi:10.1002/esp.306.
- Marshall, J. A., and L. S. Sklar (2012), Mining soil databases for landscape-scale patterns in the abundance and size distribution of hillslope rock fragments, *Earth Surf. Processes Landforms*, *37*(3), 287–300, doi:10.1002/esp.2241.
- Marshall, J. A., J. J. Roering, P. J. Bartlein, D. G. Gavin, D. E. Granger, A. W. Rempel, S. J. Praskievicz, and T. C. Hales (2015), Frost for the trees: Did climate increase erosion in unglaciated landscapes during the late Pleistocene?, *Sci. Adv.*, *1*(10e1500715), doi:10.1126/sciadv.1500715.
- Matmon, A., P. R. Bierman, J. Larsen, S. Southworth, M. Pavich, and M. Caffee (2003), Temporally and spatially uniform rates of erosion in the southern Appalachian Great Smoky Mountains, *Geology*, *31*(2), 155–158, doi:10.1130/0091-7613(2003)031<0155:TASURO>2.0.CO;2.
- Moon, S., C. Page Chamberlain, K. Blisniuk, N. Levine, D. H. Rood, and G. E. Hilley (2011), Climatic control of denudation in the deglaciated landscape of the Washington Cascades, *Nat. Geosci.*, *4*(7), 469–473, doi:10.1038/ngeo1159.
- Niemi, N. A., M. Oskin, D. W. Burbank, A. M. Heimsath, and E. J. Gabet (2005), Effects of bedrock landslides on cosmogenically determined erosion rates, *Earth Planet. Sci. Lett.*, *237*(3–4), 480–498, doi:10.1016/j.epsl.2005.07.009.
- Norton, K. P., F. von Blanckenburg, F. Schlunegger, M. Schwab, and P. W. Kubik (2008), Cosmogenic nuclide-based investigation of spatial erosion and hillslope channel coupling in the transient foreland of the Swiss Alps, *Geomorphology*, *95*(3–4), 474–486, doi:10.1016/j.geomorph.2007.07.013.
- Norton, K. P., and F. von Blanckenburg (2010), Silicate weathering of soil-mantled slopes in an active Alpine landscape, *Geochim. Cosmochim. Acta*, *74*(18), 5243–5258.
- Olen, S. M., B. Bookhagen, B. Hoffmann, D. Sachse, D. P. Adhikari, and M. R. Strecker (2015), Understanding erosion rates in the Himalayan orogen: A case study from the Arun Valley, *J. Geophys. Res. Earth Surf.*, *120*, 2080–2102, doi:10.1002/2014JF003410.
- Olivetti, V., A. J. Cyr, P. Molin, C. Faccenna, and D. E. Granger (2012), Uplift history of the Sila Massif, southern Italy, deciphered from cosmogenic ¹⁰Be erosion rates and river longitudinal profile analysis, *Tectonics*, *31*, TC3007, doi:10.1029/2011TC003037.
- Quimet, W. B., K. X. Whipple, and D. E. Granger (2009), Beyond threshold hillslopes: Channel adjustment to base-level fall in tectonically active mountain ranges, *Geology*, *37*(7), 579–582, doi:10.1130/G30013A.1.
- Palumbo, L., R. Hetzel, M. Tao, and X. Li (2010), Topographic and lithologic control on catchment-wide denudation rates derived from cosmogenic ¹⁰Be in two mountain ranges at the margin of NE Tibet, *Geomorphology*, *117*(1–2), 130–142, doi:10.1016/j.geomorph.2009.11.019.
- Portenga, E. W., and P. R. Bierman (2011), Understanding Earth's eroding surface with ¹⁰Be, *GSA Today*, *21*(8), 4–10, doi:10.1130/G1111A.1.
- Puchol, N., J. Lavé, M. Lupker, P.-H. Blard, F. Gallo, and C. France-Lanord (2014), Grain-size dependent concentration of cosmogenic ¹⁰Be and erosion dynamics in a landslide-dominated Himalayan watershed, *Geomorphology*, *224*, 55–68, doi:10.1016/j.geomorph.2014.06.019.
- Rades, E. F., R. Hetzel, M. Strobl, Q. Xu, and L. Ding (2015), Defining rates of landscape evolution in a south Tibetan graben with in situ-produced cosmogenic ¹⁰Be, *Earth Surf. Processes Landforms*, *40*(14), 1862–1876, doi:10.1002/esp.3765.
- Reinhardt, L. J., T. B. Hoey, T. T. Barrows, T. J. Dempster, P. Bishop, and L. K. Fifield (2007), Interpreting erosion rates from cosmogenic radionuclide concentrations measured in rapidly eroding terrain, *Earth Surf. Processes Landforms*, *32*(3), 390–406, doi:10.1002/esp.1415.
- Riebe, C. S., and D. E. Granger (2013), Quantifying effects of deep and near-surface chemical erosion on cosmogenic nuclides in soils, saprolite, and sediment, *Earth Surf. Processes Landforms*, *38*(5), 523–533, doi:10.1002/esp.3339.
- Riebe, C. S., J. W. Kirchner, D. E. Granger, and R. C. Finkel (2000), Erosional equilibrium and disequilibrium in the Sierra Nevada, inferred from cosmogenic ²⁶Al and ¹⁰Be in alluvial sediment, *Geology*, *28*(9), 803–806, doi:10.1130/0091-7613(2000)28<803:EEADIT>2.0.CO;2.
- Riebe, C. S., J. W. Kirchner, D. E. Granger, and R. C. Finkel (2001a), Minimal climatic control on erosion rates in the Sierra Nevada, California, *Geology*, *29*(5), 447–450, doi:10.1130/0091-7613(2001)029<0447:MCCOER>2.0.CO;2.
- Riebe, C. S., J. W. Kirchner, D. E. Granger, and R. C. Finkel (2001b), Strong tectonic and weak climatic control of long-term chemical weathering rates, *Geology*, *29*(6), 511–514, doi:10.1130/0091-7613(2001)029<0511:STAWCC>2.0.CO;2.
- Riebe, C. S., J. W. Kirchner, and R. C. Finkel (2003), Long-term rates of chemical weathering and physical erosion from cosmogenic nuclides and geochemical mass balance, *Geochim. Cosmochim. Acta*, *67*(22), 4411–4427, doi:10.1016/S0016-7037(03)00382-X.

- Riebe, C. S., J. W. Kirchner, and R. C. Finkel (2004a), Erosional and climatic effects on long-term chemical weathering rates in granitic landscapes spanning diverse climate regimes, *Earth Planet. Sci. Lett.*, *224*(3–4), 547–562, doi:10.1016/j.epsl.2004.05.019.
- Riebe, C. S., J. W. Kirchner, and R. C. Finkel (2004b), Sharp decrease in long-term chemical weathering rates along an altitudinal transect, *Earth Planet. Sci. Lett.*, *218*(3–4), 421–434, doi:10.1016/S0012-821X(03)00673-3.
- Riebe, C. S., L. S. Sklar, C. E. Lukens, and D. L. Shuster (2015), Climate and topography control the size and flux of sediment produced on steep mountain slopes, *Proc. Natl. Acad. Sci. U.S.A.*, *112*(51), 15,574–15,579, doi:10.1073/pnas.1503567112.
- Rigon, R., I. Rodriguez-Iturbe, A. Maritan, A. Giacometti, D. G. Tarboton, and A. Rinaldo (1996), On Hack's Law, *Water Resour. Res.*, *32*(11), 3367–3374, doi:10.1029/96WR02397.
- Roering, J. J., J. Marshall, A. M. Booth, M. Mort, and Q. Jin (2010), Evidence for biotic controls on topography and soil production, *Earth Planet. Sci. Lett.*, *298*(1), 183–190.
- Scherler, D., B. Bookhagen, and M. R. Strecker (2014), Tectonic control on ^{10}Be -derived erosion rates in the Garhwal Himalaya, India, *J. Geophys. Res. Earth Surf.*, *119*, 83–105, doi:10.1002/2013JF002955.
- Shreve, R. L. (1969), Stream lengths and basin areas in topologically random channel networks, *J. Geol.*, *77*(4), 397–414.
- Sklar, L. S., and W. E. Dietrich (2001), Sediment and rock strength controls on river incision into bedrock, *Geology*, *29*(12), 1087–1090, doi:10.1130/0091-7613(2001)029<1087:SARSCO>2.0.CO;2.
- Sklar, L. S., and W. E. Dietrich (2008), Implications of the saltation–abrasion bedrock incision model for steady-state river longitudinal profile relief and concavity, *Earth Surf. Processes Landforms*, *33*(7), 1129–1151, doi:10.1002/esp.1689.
- Sklar, L. S., W. E. Dietrich, E. Fofoula-Georgiou, B. Lashermes, and D. Bellugi (2006), Do gravel bed river size distributions record channel network structure? *Water Resour. Res.*, *42*, W06D18, doi:10.1029/2006WR005035.
- Sklar, L. S., C. S. Riebe, C. E. Lukens, and D. Bellugi (2016), Catchment power and the joint distribution of elevation and travel distance to the outlet, *Earth Surf. Dyn. Discuss.*, doi:10.5194/esurf-2016-9.
- Stock, G. M., T. A. Ehlers, and K. A. Farley (2006), Where does sediment come from? Quantifying catchment erosion with detrital apatite (U-Th)/He thermochronometry, *Geology*, *34*(9), 725–728, doi:10.1130/G22592.1.
- Stock, J., and W. E. Dietrich (2003), Valley incision by debris flows: Evidence of a topographic signature, *Water Resour. Res.*, *39*(4), 1089, doi:10.1029/2001WR001057.
- Strahler, A. N. (1952), Hypsometric (area-altitude) analysis of erosional topography, *Geol. Soc. Am. Bull.*, *63*(11), 1117–1142, doi:10.1130/0016-7606(1952)63[1117:HAAOET]2.0.CO;2.
- Troutman, B. M., and M. R. Karlinger (1984), On the expected width function for topologically random channel networks, *J. Appl. Probab.*, *21*(4), 836–849, doi:10.2307/3213700.
- Tucker, G. E., and K. X. Whipple (2002), Topographic outcomes predicted by stream erosion models: Sensitivity analysis and intermodel comparison, *J. Geophys. Res.*, *107*(B9), 2179, doi:10.1029/2001JB000162.
- Vance, D., M. Bickle, S. Ivy-Ochs, and P. W. Kubik (2003), Erosion and exhumation in the Himalaya from cosmogenic isotope inventories of river sediments, *Earth Planet. Sci. Lett.*, *206*(3–4), 273–288, doi:10.1016/S0012-821X(02)01102-0.
- Vassallo, R., J.-F. Ritz, and S. Carretier (2011), Control of geomorphic processes on ^{10}Be concentrations in individual clasts: Complexity of the exposure history in Gobi-Altay range (Mongolia), *Geomorphology*, *135*(1–2), 35–47, doi:10.1016/j.geomorph.2011.07.023.
- Vermeesch, P. (2007), Quantitative geomorphology of the White Mountains (California) using detrital apatite fission track thermochronology, *J. Geophys. Res.*, *112*, F03004, doi:10.1029/2006JF000671.
- von Blanckenburg, F. (2005), The control mechanisms of erosion and weathering at basin scale from cosmogenic nuclides in river sediment, *Earth Planet. Sci. Lett.*, *237*(3–4), 462–479, doi:10.1016/j.epsl.2005.06.030.
- von Blanckenburg, F., T. Hewawasam, and P. W. Kubik (2004), Cosmogenic nuclide evidence for low weathering and denudation in the wet, tropical highlands of Sri Lanka, *J. Geophys. Res.*, *109*, F03008, doi:10.1029/2003JF000049.
- Whipple, K. X., and G. E. Tucker (1999), Dynamics of the stream-power river incision model: Implications for height limits of mountain ranges, landscape response timescales, and research needs, *J. Geophys. Res.*, *104*(B8), 17,661–17,674, doi:10.1029/1999JB900120.
- White, A. F., and A. E. Blum (1995), Effects of climate on chemical weathering in watersheds, *Geochim. Cosmochim. Acta*, *59*(9), 1729–1747, doi:10.1016/0016-7037(95)00078-E.
- Wittmann, H., F. von Blanckenburg, T. Kruesmann, K. P. Norton, and P. W. Kubik (2007), Relation between rock uplift and denudation from cosmogenic nuclides in river sediment in the Central Alps of Switzerland, *J. Geophys. Res.*, *112*, F04010, doi:10.1029/2006JF000729.
- Wobus, C., A. Heimsath, K. Whipple, and K. Hodges (2005), Active out-of-sequence thrust faulting in the central Nepalese Himalaya, *Nature*, *434*(7036), 1008–1011, doi:10.1038/nature03499.
- Yanites, B. J., G. E. Tucker, and R. S. Anderson (2009), Numerical and analytical models of cosmogenic radionuclide dynamics in landslide-dominated drainage basins, *J. Geophys. Res.*, *114*, F01007, doi:10.1029/2008JF001088.